Climatic Variability and Flood Frequency of the Santa Cruz River, Pima County, Arizona

By ROBERT H. WEBB and JULIO L. BETANCOURT

Prepared in cooperation with Pima County Department of Transportation and Flood Control District

U.S. GEOLOGICAL SURVEY WATER-SUPPLY PAPER 2379

1900.017

Climatic Variability and Flood Frequency of the Santa Cruz River, Pima County, Arizona

By ROBERT H. WEBB and JULIO L. BETANCOURT

Prepared in cooperation with Pima County Department of Transportation and Flood Control District

U.S. GEOLOGICAL SURVEY WATER-SUPPLY PAPER 2379

U.S. DEPARTMENT OF THE INTERIOR
MANUEL LUJAN, JR., Secretary

U.S. GEOLOGICAL SURVEY
Dallas L. Peck, Director

Any use of trade, product, or firm names
in this publication is for descriptive purposes only
and does not imply endorsement by the U.S. Government

UNITED STATES GOVERNMENT PRINTING OFFICE, WASHINGTON : 1992

For sale by
Book and Open-File Report Sales
U.S. Geological Survey
Box 25425
Denver, CO 80225

Library of Congress Cataloging-in-Publication Data

Webb, Robert H.
Climatic variability and flood frequency of the Santa Cruz River, Pima County, Arizona / by Robert H. Webb and Julio L. Betancourt.
p. cm. — (Water-supply paper ; 2379)
Supt. of Docs. no.: I19.13:2379
Includes bibliographical references.
1. Floods—Santa Cruz River Valley (Ariz. and Mexico) 2. Floods—Arizona. 3. Hydrometeorology—Santa Cruz River Valley (Ariz. and Mexico) 4. Hydrometeorology—Arizona. I. Betancourt, Julio L. II. Title. III. Series: Geological Survey water-supply paper ; 2379
GB1399.4.S26W43 1992 92-6507
551.48'9'0979177—dc20 CIP

CONTENTS

Abstract 1
Introduction 1
Purpose and scope 3
Acknowledgments 4
Hydrologic setting 4
Hydroclimatology of southern Arizona 6
Frontal and cutoff low-pressure systems 7
Dissipating tropical cyclones 7
Monsoonal storms 7
Climatic variability in the 20th century 10
Teleconnections and 20th-century variability in global climate 11
Frequency of El Niño-Southern Oscillation conditions in the 20th century 11
Changes in circulation of the upper atmosphere 15
El Niño-Southern Oscillation and precipitation in southern Arizona 17
Hydrologic variability in the Santa Cruz River basin 17
Frequency analysis of annual floods in the Santa Cruz River 20
Previous estimates of the 100-year flood 20
Effects of land use and channel change 23
Seasonality of annual floods 23
Estimates of 100-year discharges using method of moments, 1970–85 25
Trend analysis of the annual flood series 25
Flood frequency during El Niño-Southern Oscillation conditions 26
Hydroclimatic flood-frequency analysis of the Santa Cruz River 27
Separation of floods by storm types 28
Methods of flood-frequency analysis 29
Frequency of floods caused by different storm types 32
Summary and conclusions 35
References cited 37

FIGURES

1. Map showing location of study area 2
2. Graph showing annual flood series for the Santa Cruz River at Tucson, Arizona 3
3. Graph showing average monthly streamflow and monthly streamflow variability, Santa Cruz River at Tucson, Arizona 6
4. Maps showing meteorological conditions on days during which three example floods occurred on the Santa Cruz River at Tucson, Arizona 8
5. Drawing showing schematic definitions of general circulation flow types 10

6–22. Graphs showing:
6. Seasonality of cutoff low-pressure systems over the Western United States and generation of tropical cyclones in the tropical eastern North Pacific Ocean 10
7. Variation in the number of tropical cyclones generated in the eastern North Pacific Ocean 11
8. Difference in monthly sea-level pressure between Darwin, Australia, and Tahiti 13
9. Index of Line Island precipitation 14
10. Time series of meridional and zonal flow in upper atmosphere from 1899 to 1970 16
11. Annual frequency of cutoff low-pressure systems 18

12. Correlations between the index of Line Island precipitation for the equatorial Pacific Ocean and precipitation in the Western United States **19**
13. Seasonal cumulative departures from mean discharge, Santa Cruz River at Tucson, Arizona **21**
14. Duration analyses of daily discharge for two periods, Santa Cruz River at Tucson, Arizona **22**
15. Annual flood series for six gaging stations, Santa Cruz River, southern Arizona **24**
16. Chronology of 100-year flood estimates for the Santa Cruz River at Tucson, Arizona, 1970–86 **25**
17. Chronology of moments of the log-transformed annual flood series of the Santa Cruz River at Tucson, Arizona, 1970–86 **26**
18. Comparison of flood frequency for years with and without El Niño-Southern Oscillation conditions, Santa Cruz River at Tucson, Arizona **28**
19. Largest annual floods at or above base discharge on the Santa Cruz River at Tucson caused by frontal systems, monsoonal storms, and dissipating tropical cyclones **30**
20. Mixed-population analysis of floods caused by different storm types between 1915 and 1986, Santa Cruz River at Tucson, Arizona **33**
21. Mixed-population analysis of floods caused by different storm types between 1960 and 1986, Santa Cruz River at Tucson, Arizona **34**
22. Mixed-population analysis of floods caused by different storm types between 1930 and 1959, Santa Cruz River at Tucson, Arizona **36**

TABLES

1. Annual flood series, Santa Cruz River at Tucson, Arizona **4**
2. Estimates of the 100-year flood on the Santa Cruz River at Tucson, Arizona, made by previous investigators after 1970 **5**
3. Annual flood series, Santa Cruz River at Cortaro, Arizona **6**
4. Approximate periods of El Niño-Southern Oscillation conditions in equatorial Pacific Ocean **15**
5. Matrix of correlation coefficients between Line Island monthly precipitation and Tucson monthly precipitation, 1900–82 **20**
6. Statistical properties and trend-analysis results for five periods of the annual flood series, Santa Cruz River at Tucson, Arizona **27**
7. Estimates of the 100-year flood for the Santa Cruz River calculated using different methods and based on different assumptions **29**
8. Floods above base discharge, by storm type, Santa Cruz River at Tucson, Arizona **31**
9. Floods above base discharge, by storm type, Santa Cruz River at Cortaro, Arizona **32**
10. Statistics for annual series of floods caused by three storm types for the Santa Cruz River at Tucson and Cortaro, Arizona **35**

METRIC CONVERSION FACTORS

Multiply inch pound unit	By	To obtain metric units
millimeter (mm)	0.03937	inch
meter (m)	3.2818	foot
kilometer (km)	0.6214	mile
square kilometer (km^2)	0.3861	square mile
cubic meter per second (m^3/s)	35.31	cubic foot per second
degree Celsius (°C)	°F=1.8(°C)+32	degree Fahrenheit (F°)

SEA LEVEL

In this report, "sea level" refers to the National Geodetic Vertical Datum of 1929 (NGVD of 1929)—a geodetic datum derived from a general adjustment of the first-order level net of both the United States and Canada, formerly called "Sea Level Datum of 1929."

Climatic Variability and Flood Frequency of the Santa Cruz River, Pima County, Arizona

By Robert H. Webb *and* Julio L. Betancourt

Abstract

Past estimates of the 100-year flood for the Santa Cruz River at Tucson, Arizona, range from 572 to 2,780 cubic meters per second. An apparent increase in flood magnitude during the past two decades raises concern that the annual flood series is nonstationary in time. The apparent increase is accompanied by more annual floods occurring in fall and winter and fewer in summer. This greater mixture of storm types that produce annual flood peaks is caused by a higher frequency of meridional flow in the upper-air circulation and increased variance of ocean-atmosphere conditions in the tropical Pacific Ocean.

Estimation of flood frequency on the Santa Cruz River is complicated because climate affects the magnitude and frequency of storms that cause floods. Mean discharge does not change significantly, but the variance and skew coefficient of the distribution of annual floods change with time. The 100-year flood during El Niño-Southern Oscillation conditions is 1,300 cubic meters per second, more than double the value for other years. The increase is mostly caused by an increase in recurvature of dissipating tropical cyclones into the Southwestern United States during El Niño-Southern Oscillation conditions. Flood frequency based on hydroclimatology was determined by combining populations of floods caused by monsoonal storms, frontal systems, and dissipating tropical cyclones. For 1930–59, annual flood frequency is dominated by monsoonal floods, and the estimated 100-year flood is 323 cubic meters per second. For 1960–86, annual flood frequency at recurrence intervals of greater than 10 years is dominated by floods caused by dissipating tropical cyclones, and the estimated 100-year flood is 1,660 cubic meters per second. For design purposes, 1,660 cubic meters per second might be an appropriate value for the 100-year flood at Tucson, assuming that climatic conditions during 1960–86 are representative of conditions expected in the immediate future.

INTRODUCTION

Statistical flood-frequency analysis is a commonly used method for assessing flood hazards and risks in the United States (Interagency Advisory Committee on Water Data, 1982; Thomas, 1985). This method uses the annual flood series, which is an array of the largest discharges that occur each year at a gaging station, to estimate discharges associated with various recurrence intervals, such as 10, 50, and 100 years. Certain recurrence-interval floods, such as the 100-year flood, are then used in engineering design of flood-plain structures or in managing flood plains for development. An example of the use of flood-frequency analysis is the National Flood Insurance Program, which is based primarily on the area of inundation caused by a 100-year flood (Federal Emergency Management Agency, 1986).

Flood-frequency analysis requires certain assumptions about the statistical properties of the annual flood series (Interagency Advisory Committee on Water Data, 1982). The annual flood series is assumed to be composed of random events and to be stationary in time; in other words, all floods were randomly generated from a single probability distribution with stable moments, such as the mean and variance. Thus, the floods that compose the annual flood series are assumed to be derived from the same population. Climate is assumed to be invariant, and the effects of watershed changes on flow conveyance must be negligible (Interagency Advisory Committee on Water Data, 1982). Climatic fluctuations, however, are a source of uncertainty and can lead to misjudgment and misuse of flood-frequency analyses (Dunne and Leopold, 1978, p. 311).

Many of the assumptions required for flood-frequency analysis are not routinely tested and thus could be violated. Obvious hydrologic changes commonly result from urbanization and other forms of intensified land use. Influence of climatic variability on flood frequency, however, may be subtle and more difficult to detect. Mixed populations of floods commonly occur, such as those caused by dissipating hurricanes and runoff from snowmelt. Even where this is demonstrably true, flood-frequency analysis has been used to operationally estimate flood-recurrence intervals.

The flood record for the Santa Cruz River at Tucson, Arizona (fig. 1), provides one example of an annual flood series (fig. 2; table 1) for which standard flood-frequency analyses yield inconsistent results. Past estimates of the 100-year flood for this river, using slightly different methods and lengths of record and assuming different statistical

properties of the series, range from 572 to 2,780 m^3/s (table 2). The wide range of estimates stems partially from an extraordinary flood in October 1983 (Saarinen and others, 1984) that had an estimated recurrence interval greater than 100 years (Roeske and others, 1989) and is the largest flood since 1891. Another large flood in October 1977

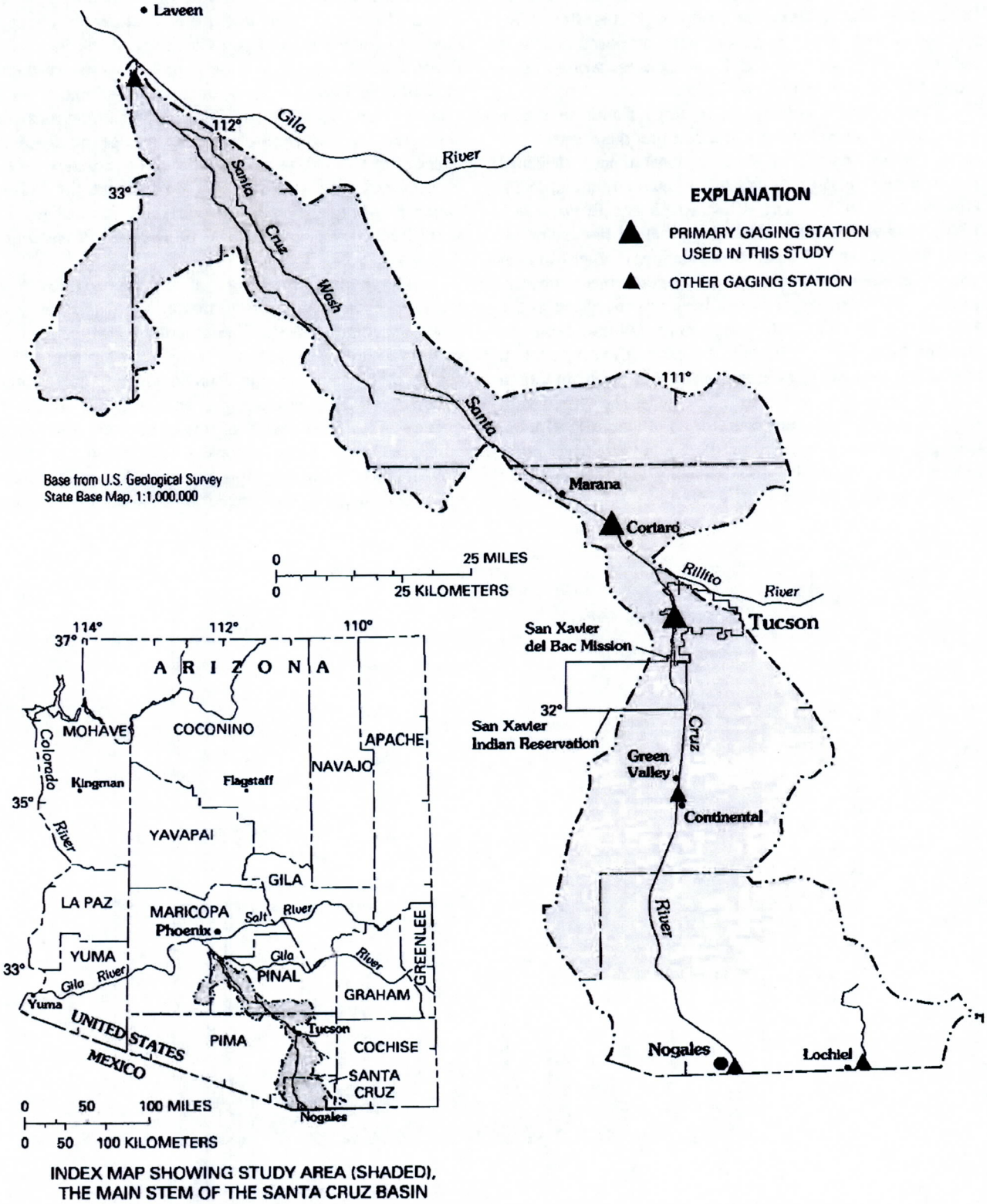

Figure 1. Location of study area (shaded).

(Aldridge and Eychaner, 1984) had a recurrence interval that, at the time, was estimated to be in excess of 100 years. Overall, six of the seven largest floods in the annual flood series (1915–86) occurred after 1960. After the 1983 flood, alternative methods for estimating design floods, including rainfall-runoff modeling, were proposed and used (Michael Zeller, Simons and Li Associates, written commun., 1984; Ponce and others, 1985).

The frequent occurrence of large floods in recent years has led several authors to assert that the annual flood series for the Santa Cruz River is nonstationary (Michael Zeller, Simons and Li Associates, written commun., 1984; Hirschboeck, 1985; Baker, 1984; Reich and Davis, 1985, 1986), thus violating the assumption that all floods are derived from the same statistical population. Changes in land use have been blamed for the alleged nonstationarity (Reich, 1984), but larger floods have also occurred in the headwaters of the Santa Cruz River, where land-use changes have been negligible. An alternative explanation is that low-frequency shifts in climate that occur on a time scale of decades have led to a change in the type, intensity, and (or) frequency of storms that cause floods. Changes in flood frequency on the Santa Cruz River coincide with apparent shifts in seasonality and magnitude of floods elsewhere in the Gila River basin.

Purpose and Scope

In 1988, the U.S. Geological Survey in cooperation with Pima County Department of Transportation and Flood Control District undertook a study of changing channel conditions and flood frequency of the Santa Cruz River. Part of this larger study is an assessment of the applicability of flood-frequency analysis in estimating the recurrence intervals of floods. Whereas much previous work addressed the influence of channel change on flood frequency, this report uses the hydroclimatic perspective of Hirschboeck (1985, 1987, 1988) to evaluate the link between low-frequency climatic variability and changes in flood frequency of the Santa Cruz River in Pima County, Arizona.

The hydroclimatology of the Santa Cruz River basin is examined with particular emphasis on storm types that cause floods. The extent of 20th-century climatic variability is analyzed using long-term records of sea-level pressure in the Pacific Ocean, upper atmospheric circulation patterns, and tropical-storm frequency. The time series of these climatic indices are compared with weather records from Tucson and streamflow records from the gaging station, Santa Cruz River at Tucson, to show the connection between climatic vari-

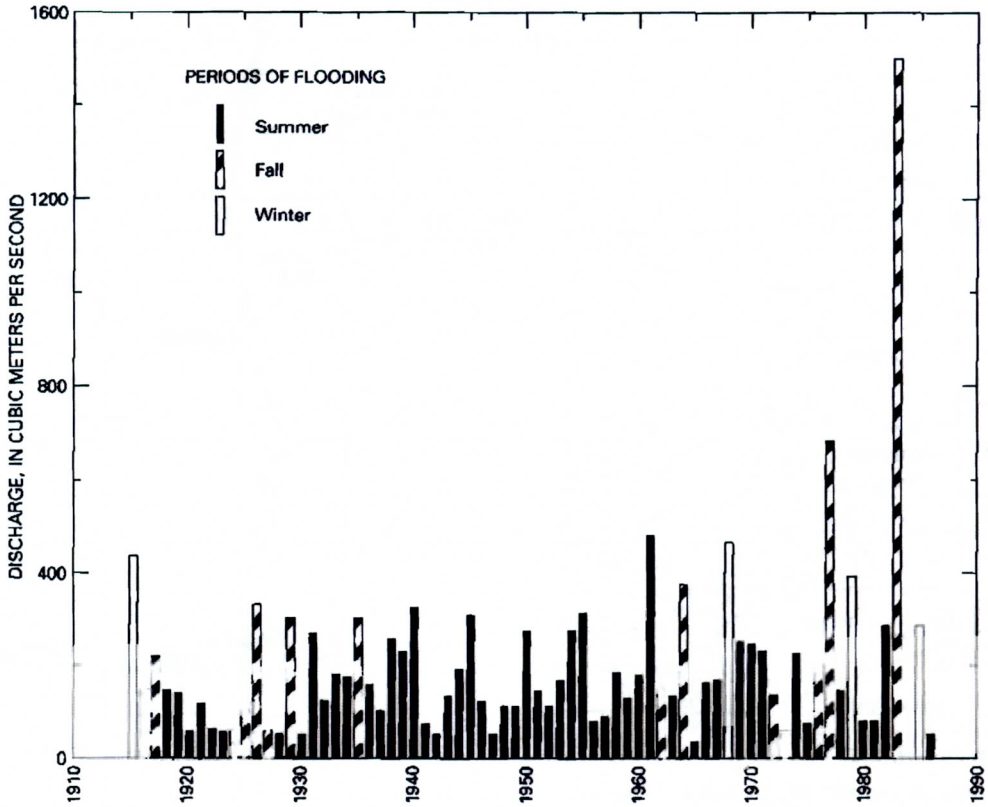

Figure 2. Annual flood series for the Santa Cruz River at Tucson, Arizona. Hydroclimatological year is November 1 to October 31.

Table 1. Annual flood series, Santa Cruz River at Tucson, Arizona

[Water year for annual flood series, November 1 to October 31]

Date	Discharge, in cubic meters per second	Date	Discharge, in cubic meters per second	Date	Discharge, in cubic meters per second
12-23-14	425	8-03-39	227	8-26-63	132
1-20-16	142	8-14-40	320	9-10-64	368
9-08-17	212	8-14-41	71	7-16-65	34
8-07-18	139	8-09-42	47	8-19-66	156
8-02-19	133	8-02-43	128	7-17-67	166
8-09-20	55	8-16-44	185	12-20-67	456
8-01-21	113	8-10-45	306	8-06-69	247
7-20-22	57	8-04-46	121	7-20-70	242
8-17-23	54	8-10-47	48	8-17-71	227
11-17-23	58	8-16-48	109	10-19-72	133
9-18-25	96	8-08-49	108	3-14-73	54
9-28-26	323	7-30-50	269	7-08-74	225
9-07-27	55	8-02-51	142	7-12-75	70
8-01-28	45	8-16-52	108	9-25-76	201
9-24-29	295	7-15-53	167	10-10-77	671
8-07-30	50	7-24-54	271	8-02-78	142
8-10-31	261	8-03-55	309	12-19-78	382
7-30-32	119	7-29-56	74	8-13-80	78
8-21-33	173	8-31-57	86	7-27-81	76
8-23-34	170	7-29-58	180	8-23-82	[1]283
9-01-35	292	8-20-59	125	10-02-83	1,493
7-26-36	153	8-10-60	174	12-28-84	283
7-10-37	93	8-23-61	470	7-21-86	54
8-05-38	255	9-26-62	141		

[1]Estimated.

ability and hydroclimatology of southern Arizona. Also examined is the influence of climatic variability on the frequency and severity of storm types that cause flooding in southern Arizona. Flood frequency is analyzed using several different methods and assumptions about the data that are based on the hydroclimatic analysis. A mixed-population analysis made on the basis of hydroclimatic segregation of floods and maximum-likelihood analysis is used to estimate flood frequency for floods caused by different storm types in different periods of the 20th century.

Acknowledgments

Ellen Wohl of the Colorado State University, T.W. Swetnam and H.C. Fritts of the University of Arizona, D.R. Cayan of the Scripps Institution of Oceanography, and A.V. Douglas of Creighton University provided some of the climatic data used in this report. Much of this research was inspired by the work of Walter Smith (Smith, 1986) and especially the work of K.K. Hirschboeck (Hirschboeck, 1985, 1987, 1988), both of the University of Arizona. Discussions with Smith and Hirschboeck helped us extend their work in this study. K.C. Young of the University of Arizona gave access to his collection of National Oceanic and Atmospheric Administration Daily Weather Maps, and D.R. Cayan provided office space and logistical support at Scripps Institution of Oceanography.

Hydrologic Setting

The Santa Cruz River is primarily an ephemeral desert stream and drains 22,200 km^2 in southern Arizona and northern Mexico. From its headwaters in the mountains of southern Arizona, the river flows southward into Mexico and loops north to re-enter the United States just east of Nogales. The river flows 105 km from Nogales to Tucson (fig. 1). During major floods, the Santa Cruz River below Tucson flows another 155 km to join the Gila River near Phoenix; however, this reach is typically dry or contains treated sewage or irrigation-return flow. The headwaters of the Santa Cruz are at an altitude of 2,885 m above sea level, the confluence with the Gila River occurs at 310 m, and the average basin altitude above Tucson is 1,234 m above sea level (Roeske, 1978). The basinwide precipitation for the Santa Cruz River basin is 430 mm/yr. Several large historic floods

Table 2. Estimates of the 100-year flood on the Santa Cruz River at Tucson, Arizona, made by previous investigators after 1970

[———, no record]

Reference	Years of record	Method or probability distribution	100-year flood, in cubic meters per second
U.S. Army Corps of Engineers (1972)	———	([1])	1,280
Roeske (1978)	1915–75	([2])	575
	1915–75	([3])	640
Malvick (1980)	1915–78	([3])	1,810
Federal Emergency Management Agency (1982)	1915–78	([2])	850
Boughton and Renard (1984)	1915–79	([4])	572
	1915–79	([2])	666
	1915–79	([5])	2,180
Michael Zeller (Simons and Li Associates, written commun., 1984)	———	([6])	1,420
Eychaner (1984)	1915–81	([2])	626
	1915–81	([3])	657
Reich (1984)	1960–84	([2])	1,530
	1960–84	([7])	2,730
	1962–84	([2])	1,420
	1962–84	([7])	2,780
Ponce and others (1985)	———	[8]24	1,660
		[8]48	1,900
		[8]96	1,330
Hirschboeck (1985)	1950–80	([2])	736

[1]Curve, comparison with floods in other watersheds in southern Arizona.
[2]Log-Pearson type III distribution, method-of-moments fitting.
[3]Log-Pearson type III distribution plus regression analysis.
[4]Log-Pearson type III distribution plus envelope curve.
[5]Log-Boughton distribution, method-of-moments fitting.
[6]Rain, estimated from 100-year rainfall.
[7]Log-Extreme Value distribution, method-of-moments fitting.
[8]Model, estimated from rainfall-runoff model with 100-year, 24-, 48-, and 96-hour duration storms. This value is currently being used by Pima County for compliance with Federal Emergency Management Agency regulations.

on the Santa Cruz River have been described previously (Knapp, 1937; Lewis, 1963; Aldridge, 1970; Aldridge and Eychaner, 1984; Saarinen and others, 1984; Roeske and others, 1989).

Three long-term gaging stations have been maintained on the Santa Cruz River in Pima County. The gaging record for the Santa Cruz River at Tucson is the longest but is discontinuous because of a complicated station history. Although the first gaging station was installed in 1905 (Schwalen, 1942), the continuous gaging record began in 1915. The station was discontinued in 1981 and was re-established in 1986 (Wilson and Garrett, 1989). In this report, streamflow records for 1915-86 were evaluated, and annual peak discharges were measured or estimated for all years during 1915–86 (fig. 2; table 1). Peaks above a base discharge of 48 m^3/s (the partial-duration series) were measured for 1930–81; however, peaks above base discharge are not known for July and August 1984 or for water year 1985. The mean annual streamflow is 0.64 m^3/s at Tucson from a drainage area of 5,755 km^2 (Wilson and Garrett, 1989).

The gaging station, Santa Cruz River at Cortaro, Arizona (fig. 1), has a record from 1939–47 and 1950–84, after which the station was discontinued (White and Garrett, 1987). The drainage area above this gaging station is 9,073 km^2. Discharges for both the annual flood series (table 3) and the partial-duration series are available for all years of record. The base discharge for the partial-duration series is 76 m^3/s. A record from the gaging station, Santa Cruz River at Continental, Arizona, was not analyzed for flood frequency. Discharges for many floods at this gaging station are inaccurate because flow in an overflow channel around the gaging station was not measured (H.W. Hjalmarson, hydrologist, U.S. Geological Survey, oral commun., 1989).

Averages of monthly discharge for the Santa Cruz River at Tucson indicate that runoff occurs mainly from

Table 3. Annual flood series, Santa Cruz River at Cortaro, Arizona

[Water year for annual flood series, November 1 to October 31]

Date	Discharge, in cubic meters per second	Date	Discharge, in cubic meters per second
8-14-40	481	8-26-63	205
12-31-40	221	9-10-64	450
8-09-42	43	12-22-65	475
9-24-43	155	8-19-66	169
8-16-44	160	7-17-67	162
8-10-45	396	12-21-67	447
8-04-46	125	8-06-69	238
8-15-47	212	7-20-70	317
7-30-50	365	8-20-71	257
7-25-51	193	10-19-72	255
8-14-52	172	2-22-73	104
7-14-53	305	7-08-74	331
7-24-54	259	7-12-75	147
8-03-55	470	9-25-76	300
7-29-56	89	10-10-77	651
9-01-57	124	3-02-78	221
9-01-57	124	12-18-78	532
8-12-58	223	7-19-80	75
8-20-59	226	9-22-81	122
8-11-60	181	8-23-82	376
8-23-61	416	10-02-83	1,841
9-26-62	317	8-16-84	145

December through February and July through October (fig. 3). Variability in monthly streamflow is high, and coefficients of variation range from 1 to 6 (fig. 3). Because the normally defined water year of October 1 to September 30 artificially separates the fall runoff season, a hydroclimatic water year was defined for this report as November 1 to October 31. Redefinition of the water year, which satisfies the assumption of interannual independence in annual floods, shifts some floods that occur in October, such as the flood of October 1983, to the previous water year.

Precipitation in southern Arizona has distinct peaks in summer and winter (Sellers and Hill, 1974). Tucson has one of the longest precipitation records (1868–1989) in Arizona, although, like other long-term southwestern stations, it has a complicated station history (Durrenberger and Wood, 1979). The University of Arizona has maintained precipitation records since 1891, although the station has been moved to five locations within a 15-kilometer radius. There were major station moves in 1894, 1956, 1966, and 1968; the effect of these moves on the statistical properties of the time series has not been determined. Mean annual precipitation recorded at the University of Arizona in Tucson is 291 mm for the 119-year record. About 129 mm of rain falls between November and June, and 162 mm of rain falls between July and October.

The predominant land use is for livestock grazing, which has occurred for several centuries. Bottomlands are used for agriculture, primarily alfalfa and pecans. Copper is mined in several areas of the drainage basin, mainly near Green Valley, Arizona (fig. 1). Urbanization affects Nogales, Sonora, in Mexico; and Nogales, Green Valley, Tucson, and Marana in Arizona. Green Valley and Tucson incorporate flood-prone properties along the Santa Cruz River.

HYDROCLIMATOLOGY OF SOUTHERN ARIZONA

Recent hydroclimatological research in southern Arizona links various flood-producing storm types to large-scale atmospheric-oceanic interactions (Hansen and others, 1977; Maddox and others, 1980; Hansen and Schwarz, 1981; Hirschboeck, 1985, 1987; Smith, 1986). Three principal types of flood-producing storms and associated upper-atmospheric circulation patterns are described below.

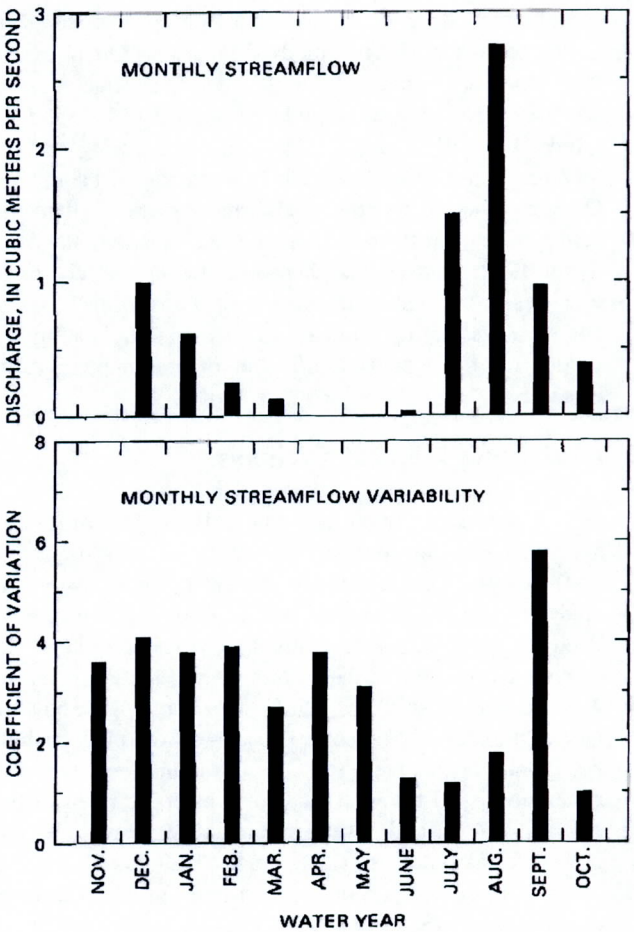

Figure 3. Average monthly streamflow and monthly streamflow variability, Santa Cruz River at Tucson, Arizona.

Frontal and Cutoff Low-Pressure Systems

Winter storms in southern Arizona originate from large-scale low-pressure frontal systems embedded in the westerly winds from the Pacific Ocean. The storm track moves southward in conjunction with seasonal expansion of a low-pressure cell, called the Aleutian Low, that occurs in the North Pacific. During dry winters, the westerlies follow a path around the north side of a ridge of high pressure off the west coast of North America and into the Pacific Northwest. In wet winters, this ridge is displaced westward, and a low-pressure trough develops over the Western United States. Storms then tend to follow the prevailing winds along the west coast and enter the continent as far south as San Francisco. An example of a frontal system that caused a flood on the Santa Cruz River is the storm of December 17–18, 1978 (fig. 4*A*, *B*). The rainfall during this storm ranged from 70 to 250 mm in central Arizona and caused widespread flooding (Aldridge and Hales, 1984).

When a high-pressure ridge in the Pacific is well developed, low-pressure systems can stagnate and form cutoff low-pressure systems (fig. 5). The atmospheric conditions that produce cutoff low-pressure systems are discussed in the section titled "Changes in Circulation of the Upper Atmosphere." Cutoff lows that affect Arizona typically form between latitude 30° N. and 45° N. and longitude 105° W. and 125° W. and have spring and fall maxima (fig. 6). Cutoff lows may intensify off the coast of California before moving inland into Arizona, where they can produce substantial rainfall (Sellers and Hill, 1974; Pyke, 1972; Hansen and Schwarz, 1981). In fall, cutoff low-pressure systems may stall over warm tropical waters and steer dissipating tropical cyclones inland, creating conditions for the idealized probable-maximum precipitation in Arizona (Hansen and Schwarz, 1981).

Dissipating Tropical Cyclones

Occasionally in late summer and early fall, widespread and intense rainfall occurs in southern Arizona because of northeastward penetration of tropical cyclones, which include hurricanes and tropical storms, from the tropical North Pacific Ocean. An average of 14.1 tropical cyclones are generated each year in the eastern North Pacific Ocean (fig. 7; Rosendal, 1962; Cross, 1988). July and August have the largest number of tropical cyclones—3.4 and 3.5 cyclones per month, respectively (fig. 6). The main area of cyclone generation is off the west coast of Mexico between latitude 10° and 15° N. and between longitude 95° and 100° W.; most tropical cyclones originate more than 300 km south of Cabo San Lucas, the southernmost point in Baja California (Eidemiller, 1978; Cross, 1988).

After leaving their area of origin, most tropical cyclones curve west-northwestward and may intensify into tropical storms or hurricanes. Farther north and west, the storms are dissipated by wind shear and colder water. Some tropical cyclones recurve toward the north and east, steered either by southerly winds ahead of a low-pressure trough, centered over the Pacific Northwest, by a weak trough between two subtropical high-pressure cells, or by circulation associated with a cutoff low-pressure system. These cyclones dissipate over Mexico and the United States, causing intense precipitation and regional flooding (Smith, 1986). Precipitation from dissipating tropical cyclones can range from several millimeters to more than 300 mm in 2 to 4 days (Smith, 1986).

Recurving cyclones that have affected southern Arizona were generated most frequently in September and October—72 percent—compared with July and August—27 percent (Smith, 1986). Between 1965 and 1984, an average of 1.4 tropical cyclones per year caused precipitation in the Southwestern United States (Smith, 1986). Tropical Storm Octave in late September and early October 1983 is an example of the interaction between a tropical cyclone and a cutoff low-pressure system (fig. 4*C*) that caused flooding on the Santa Cruz River (Roeske and others, 1989).

The disparity between seasonality of cutoff low-pressure systems and generation of tropical cyclones explains the greater incidence of recurvature during fall (fig. 6). Although generation of tropical cyclones is at a maximum in July and August, cutoff low-pressure systems have a maximum incidence in October. The greater incidence of recurvature in fall also is associated with the weakening and southern migration of the Pacific subtropical high and the more frequent appearance of midlatitude troughs at lower latitudes (Eidemiller, 1978). These two phenomena can behave synergistically, because dissipating tropical cyclones may contribute moisture to early fall extratropical cyclones from the North Pacific.

Monsoonal Storms

The summer rainy season in Arizona is preceded by strong zonal flow and aridity under direct influence of subsidence from the subtropical high-pressure cell in the eastern Pacific Ocean, which remains displaced to the south during spring and early summer. Near the end of June and early July, the subtropical high-pressure cells shift rapidly northward and induce advection of moist tropical air into Arizona. These synoptic-scale surges (Carleton, 1986) that abruptly break the early summer drought have been likened to monsoonal circulation elsewhere (Tang and Reiter, 1984). The resultant monsoonal storms are characterized by isolated or complex groups of thunderstorms that have a duration of less than several hours (Maddox and others, 1980; Hansen and Schwarz, 1981). Analyses of broad-scale patterns in precipitable water (Reitan, 1960), water-vapor flux

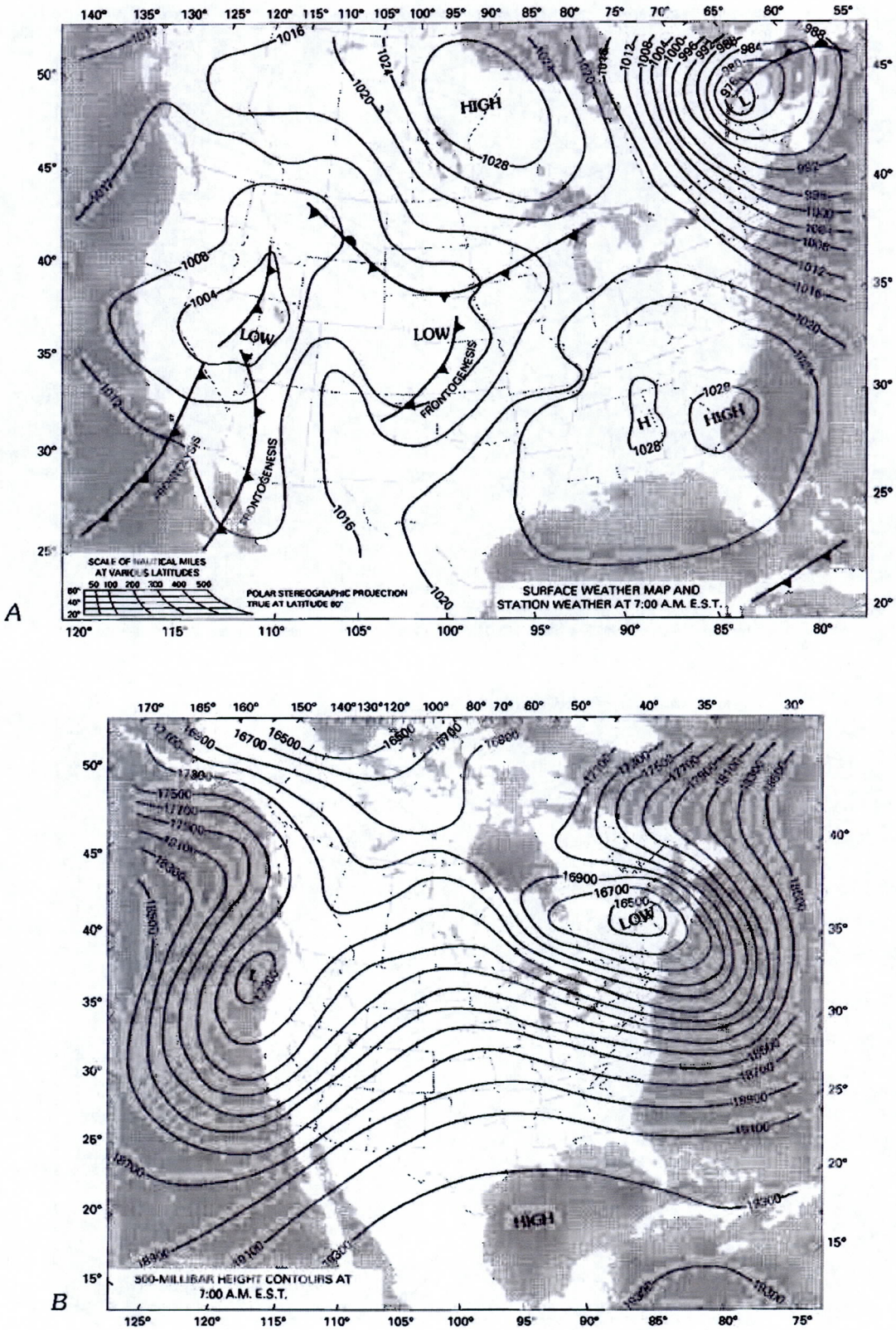

Figure 4. Meteorological conditions on days during which three example floods occurred on the Santa Cruz River at Tucson, Arizona. (Maps from the Daily Weather Map series of the National Oceanic and Atmospheric Administration, 1988.) *A*, A frontal system passed through Arizona on December 18, 1978. Contours in millibars. *B*, On December 18, 1978, a large low-pressure trough off the California coast was associated with the frontal system shown in *A*. Contours in feet above

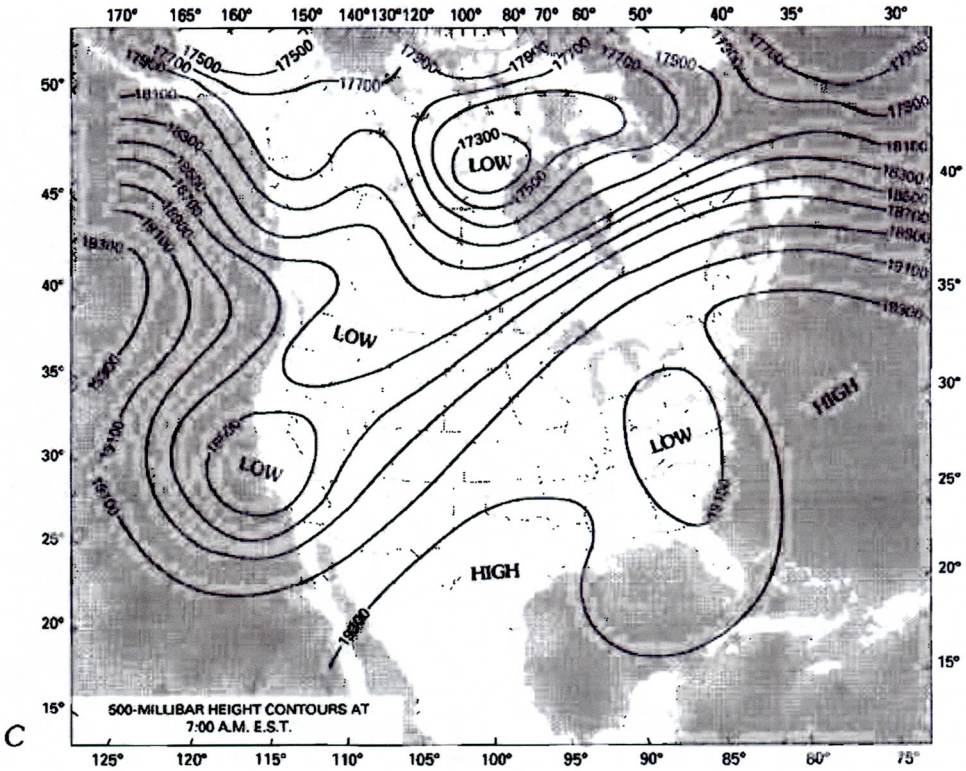

C

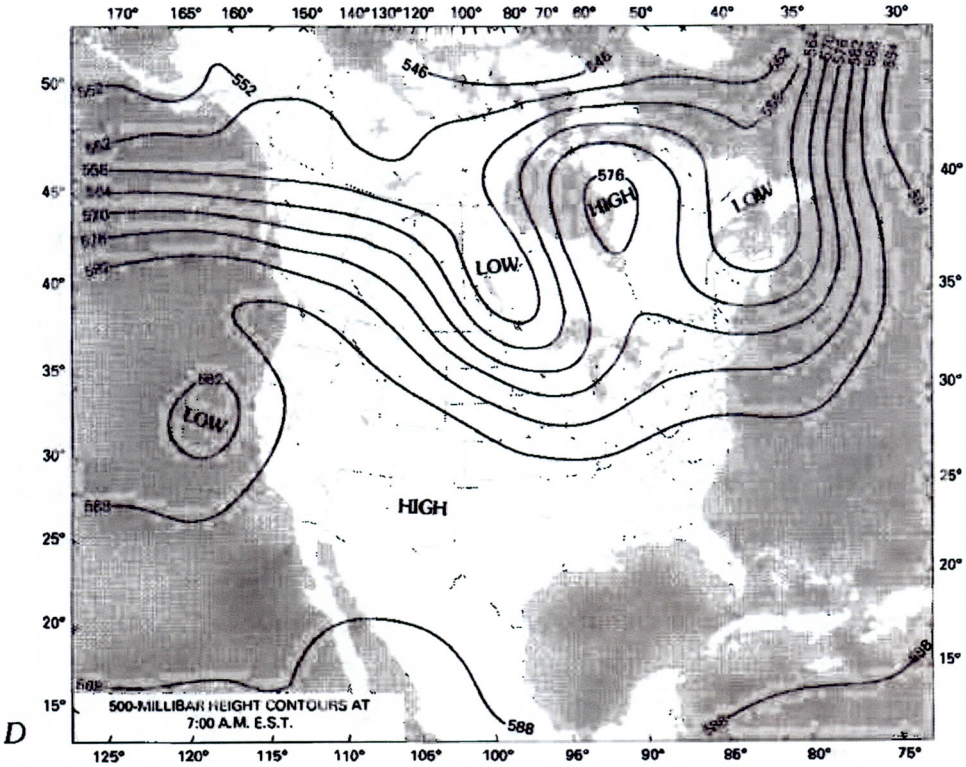

D

sea level. *C*, On October 1, 1983, a cutoff low-pressure system was over the California coast. At the same time, Tropical Storm Octave was off the southwestern tip of Baja California. Contours in feet above sea level. *D*, On August 23, 1988, generally weak upper atmospheric conditions were associated with monsoonal precipitation in Arizona. Contours in tens of meters above sea level.

(Rasmusson, 1967), low-level winds (Tang and Reiter, 1984), and regional precipitation (Hales, 1974; Pyke, 1972) suggest that much of the moisture originates from the Pacific Ocean and Gulf of California. Hansen and Schwarz (1981) asserted that although the Gulf of Mexico may be the source for much of the day-to-day summer precipitation in the Southwest, it is not the source of moisture for extreme precipitation. Floods caused by monsoonal storms have occurred in almost every year of record for the Santa Cruz River. An example of the weak upper-atmospheric circulation of a typical monsoonal storm occurred on August 23, 1988 (fig. 4*D*). This storm dropped about 70 mm of rainfall in 1 hour in parts of southwestern Tucson.

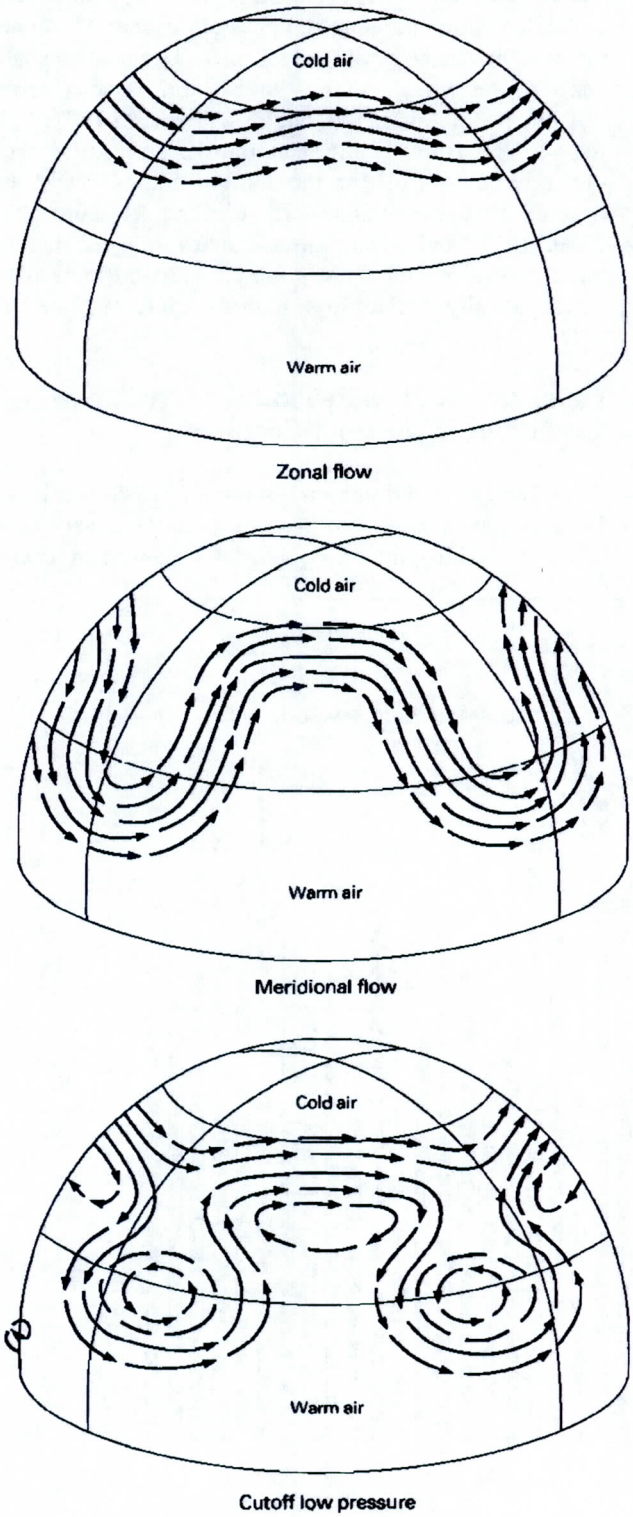

Figure 5. Schematic definitions of general circulation flow types.

CLIMATIC VARIABILITY IN THE 20TH CENTURY

Large-scale climatic phenomena affect the hydroclimatology of southern Arizona and the watershed of the Santa Cruz River. Location of the watershed in a climatic transition zone between temperate and tropical latitudes contributes to distinct seasonal precipitation and streamflow. Streamflow may be a less ambiguous measure of climatic variability than precipitation because it integrates weather phenomena over space and time. In large watersheds such as the Santa Cruz River basin, floods often occur under a special set of climatic conditions that combine general circulation over North America and sea-surface temperatures in the Pacific Ocean (Hansen and others, 1977). Thus, floods can integrate climatic information that might be difficult to detect in more direct measurements of the climate system.

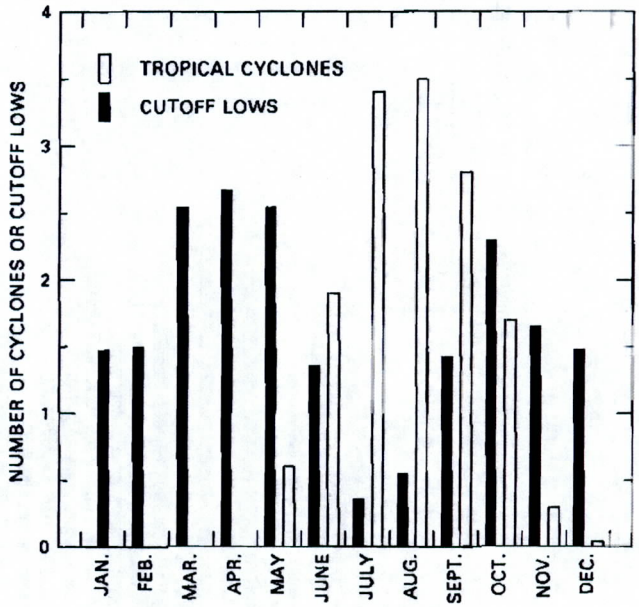

Figure 6. Seasonality of cutoff low-pressure systems over the Western United States (lat 20° to 45° N., long 100° to 140° W.) and generation of tropical cyclones in the tropical eastern North Pacific Ocean (lat 5° to 20° N., long 85° to 120° W.).

Teleconnections and 20th-Century Variability in Global Climate

Precipitation patterns in certain parts of the world are teleconnected, or related over long distances (Ropelewski and Halpert, 1986). For example, the Southwestern United States occasionally has abundant precipitation while the Northwestern United States undergoes drought (Lins, 1985). Similarly, the Southeastern United States and much of northern South America are negatively teleconnected. Propagation of teleconnections worldwide suggests that the same climatic process may control concurrent flooding in Arizona and Florida or in India and Australia.

Teleconnections provide a network for studying the worldwide propagation of low-frequency climatic fluctuations. Using precipitation as an example, summer rainfall in the positively teleconnected areas of India (Mooley and Parthasarathy, 1984), west Africa (Ojo, 1987), and the Sahel (Folland and others, 1986) was above normal for 1930–60 and below normal before and after 1930–60. Changes in ocean temperatures appear to precede the changes in precipitation. In the Atlantic Ocean, warming occurred in the Southern Hemisphere and cooling occurred in the Northern Hemisphere before about 1925 and after the late 1950's to early 1960's (Folland and others, 1986; Cayan, 1986). The Pacific Ocean also cooled after the early 1960's. This cooling coincided with anomalous upper-atmospheric pressure patterns in the central North Pacific Ocean and southward displacement of the winter storm tracks across western North America (Douglas and others, 1982; Balling and Lawson, 1982). Cumulative departures from mean temperatures for the United States (Diaz and Quayle, 1980) show significant breakpoints about 1921, 1930, 1952, and 1960. These studies suggest that the middle third of this century (about 1930–60) appears to be climatically distinct from periods before 1930 or after 1960.

Frequency of El Niño-Southern Oscillation Conditions in the 20th Century

The El Niño-Southern Oscillation (ENSO) involves the appearance every 3 to 5 years of anomalously warm water (El Niño) in the equatorial eastern and central

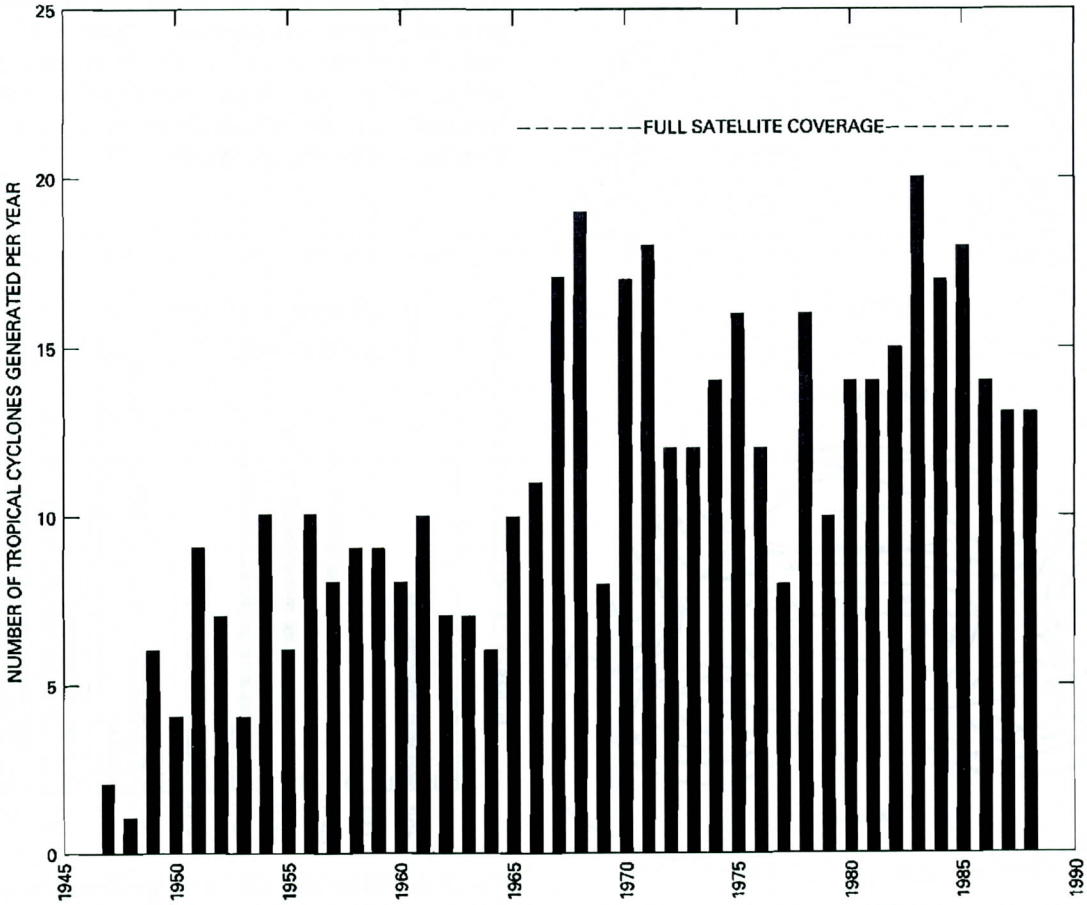

Figure 7. Variation in the number of tropical cyclones generated in eastern North Pacific Ocean between lat 5° N. and 20° N. and long 85° W. and 120° W. Tropical cyclones include hurricanes and tropical storms. Full detection began after 1965 with daily satellite coverage (data from Cross, 1988).

Pacific (Rasmusson, 1985; Enfield, 1989). During ENSO events, the sea-surface temperature anomalies are accompanied by unusually high sea-level pressure near Indonesia and unusually low sea-level pressure near the central equatorial Pacific Ocean (Rasmusson, 1984). The term "La Niña" refers to anomalous cooling in the equatorial Pacific (Bradley and others, 1987). ENSO affects various meteorological and oceanographic conditions worldwide. Teleconnections are particularly pronounced during ENSO conditions (Horel and Wallace, 1981; Elliott and Angell, 1988).

Several indices have been developed that indicate ENSO conditions. The difference in sea-level pressure between Darwin, Australia, and Tahiti (fig. 8) is commonly used to create an index of the Southern Oscillation. The pressure difference has a significant month-to-month persistence, as indicated by serial autocorrelation coefficients that are significantly different from zero for 8 months. Several variations of this index have been developed (Troup, 1965; Wright, 1984; Ropelewski and Jones, 1987). The most common, the Southern Oscillation Index (SOI), is the pressure difference between Darwin and Tahiti normalized to a mean of zero and a variance of one (Ropelewski and Jones, 1987). Negative values of the Darwin-Tahiti pressure difference indicate ENSO conditions.

Precipitation in the Line Islands of the equatorial Pacific Ocean (lat 0° to 10° N., long 160° W.) also has been used as an index of ENSO conditions. Distinct precipitation surges occur in these normally dry islands under ENSO conditions (Wright, 1984; Douglas and Englehart, 1984). Positive values of the index of Line Island precipitation (fig. 9) indicate ENSO conditions. This index is significantly autocorrelated for 7 months, similar to the Darwin-Tahiti pressure difference. Fewer surges of precipitation occurred in the Line Islands during 1930–63 (Reiter, 1983).

One of the problems in analyses of ENSO-related phenomena is the use of different criteria for identifying ENSO conditions, such as sea-surface temperatures in Peru, several versions of the SOI, or Line Island precipitation. When there is a high negative correlation between sea-surface temperature in the eastern Pacific Ocean and the SOI, strong ENSO years are easily defined. Differences arise when defining weaker ENSO years because warming occurs without a large reversal in sea-surface pressure. The Darwin-Tahiti pressure difference and the Line Island precipitation index were used to develop a chronology of 20th-century ENSO conditions (table 4). The chronology differs only slightly from existing chronologies of ENSO (table 4), does not have a denotation of strength, and gives the approximate beginning and ending times for ENSO conditions.

Using the classification in table 4, ENSO conditions recurred on the average of every 3.8 years for 1900–29, every 4.3 years for 1930–59, and every 3.8 years for 1960–86. The seasonality during which ENSO conditions are present has changed during the 20th century. For 1930–60, ENSO conditions often began in the early part of the year and ended in the late part of the year, and the interval between ENSO conditions was as long as 7 years (table 4). Between 1960 and 1986, ENSO conditions typically began in the middle of the year and lasted until the early or middle part of the following year, and the longest interval between ENSO conditions was 5 years (table 4).

Changes in the statistical properties of the Darwin-Tahiti pressure difference (fig. 8) reflect decadal changes in ENSO conditions. The mean pressure difference is 0.3 millibar (mbar) for 1930–59 and –0.2 mbar for 1960–86. Although the means are not significantly different, the intermonthly variance in sea-level pressure increased from 43 mbar during 1930–59 to 60 mbar after 1960. The increase in variance after 1960 is statistically significant at a 95-percent confidence level using the nonparametric Squared Ranks Test (Conover, 1971, p. 239–241). Elliott and Angell (1988) also found reduced variances in sea-level pressure at Darwin and Tahiti for about 1920–50. The increased frequency of ENSO conditions suggests an increased occurrence of high sea-surface temperatures, which may affect the occurrence and (or) intensity of frontal storms in the extratropical latitudes.

Precipitation in the Line Islands shows seasonal changes after 1960. Average precipitation from August through February increased after 1960. For September through December, the increases ranged from 12 to 23 percent. The mean for 1960–82 is only 6 percent greater than the record mean; however, the mean for 1976–82 of 127 percent of normal precipitation illustrates the persistent ENSO conditions during this period. This scenario is consistent with the virtual absence, without precedent in the 20th century, of La Niña conditions during 1975–87 (Bradley and others, 1987).

ENSO conditions affect the hydroclimatology of the southwestern United States, particularly Arizona (Andrade and Sellers, 1988; Douglas and Engelhart, 1984). Areas teleconnected with the equatorial Pacific Ocean, such as the Southwestern United States, have increased variability of precipitation (Nicholls, 1988). Winter frontal storms are more numerous and intense during certain ENSO years (Rasmusson, 1984, 1985) because of an intensified Aleutian low (Yarnal and Diaz, 1986). The probabilities for generation and recurvature of tropical cyclones change during ENSO conditions, but the advection of moisture needed to fuel monsoonal storms is reduced (Reyes and Cadet, 1988). Hypothetically, ENSO conditions could reduce the number of monsoonal storms but increase the number of frontal systems and tropical cyclones that affect Arizona.

ENSO affects the variability of tropical-cyclone generation. After 1965, all tropical cyclones generated in the eastern North Pacific Ocean were detected by weather satellites. On average, fewer tropical cyclones were generated

under ENSO conditions (12.6 tropical cyclones per year) than under non-ENSO conditions (15.3 tropical cyclones per year). Analysis of variance, however, indicates a significant difference at the 95-percent confidence level between the variances of generation of tropical cyclones during ENSO and non-ENSO conditions. The incidence of

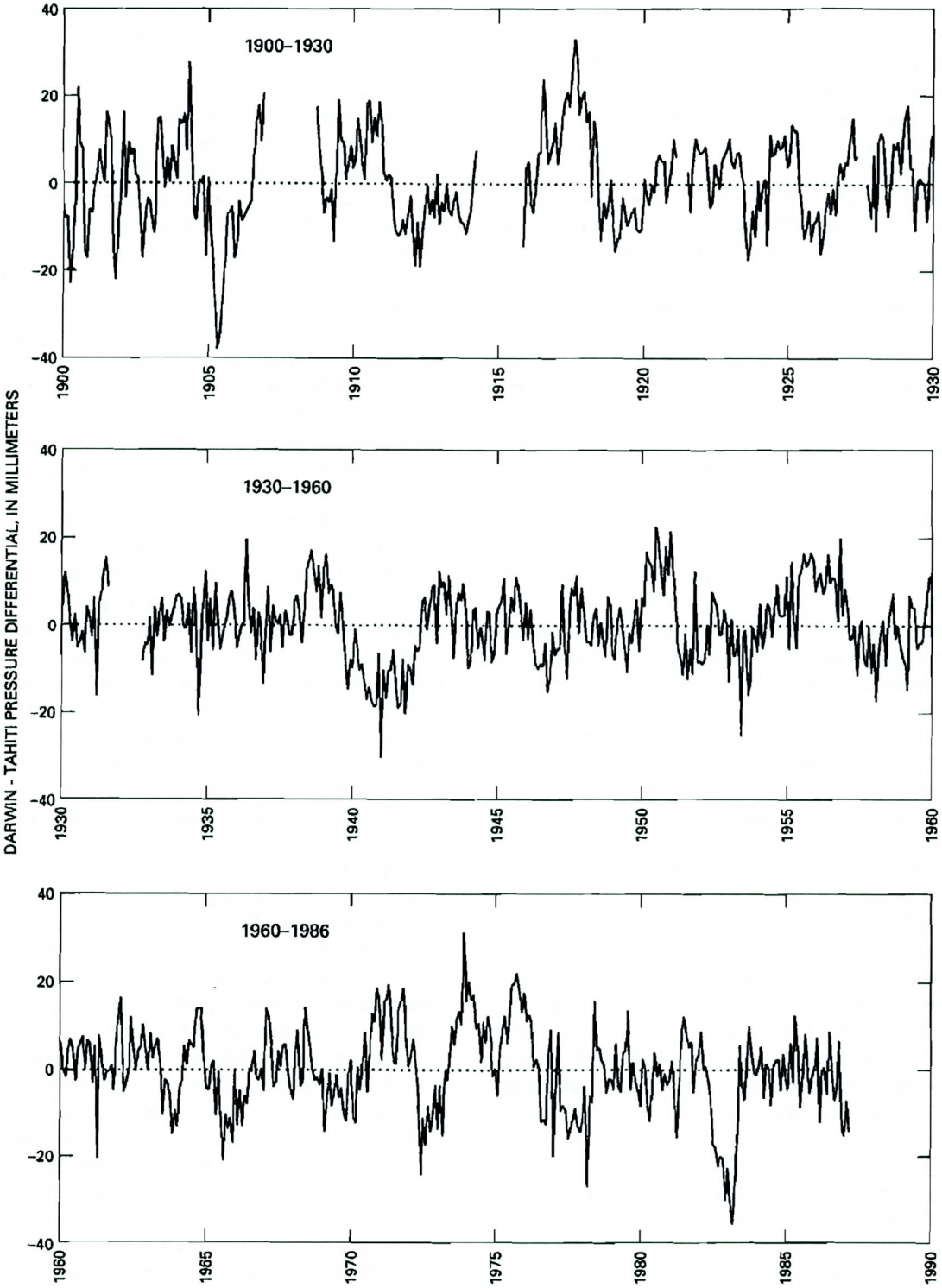

Figure 8. Difference in monthly sea-level pressure between Darwin, Australia, and Tahiti. Sea-level pressure difference is a measure of El Niño-Southern Oscillation conditions; negative values indicate warm El Niño-Southern Oscillation conditions.

tropical cyclones dissipating over Arizona increases during ENSO conditions. The largest numbers of dissipating tropical storms per year that affected the Southwestern United States occurred in the ENSO years of 1925–26, 1939, 1957–58, 1976–77, and 1982–83 (Smith, 1986). In September, the peak month for recurvature, 3.4 tropical cyclones

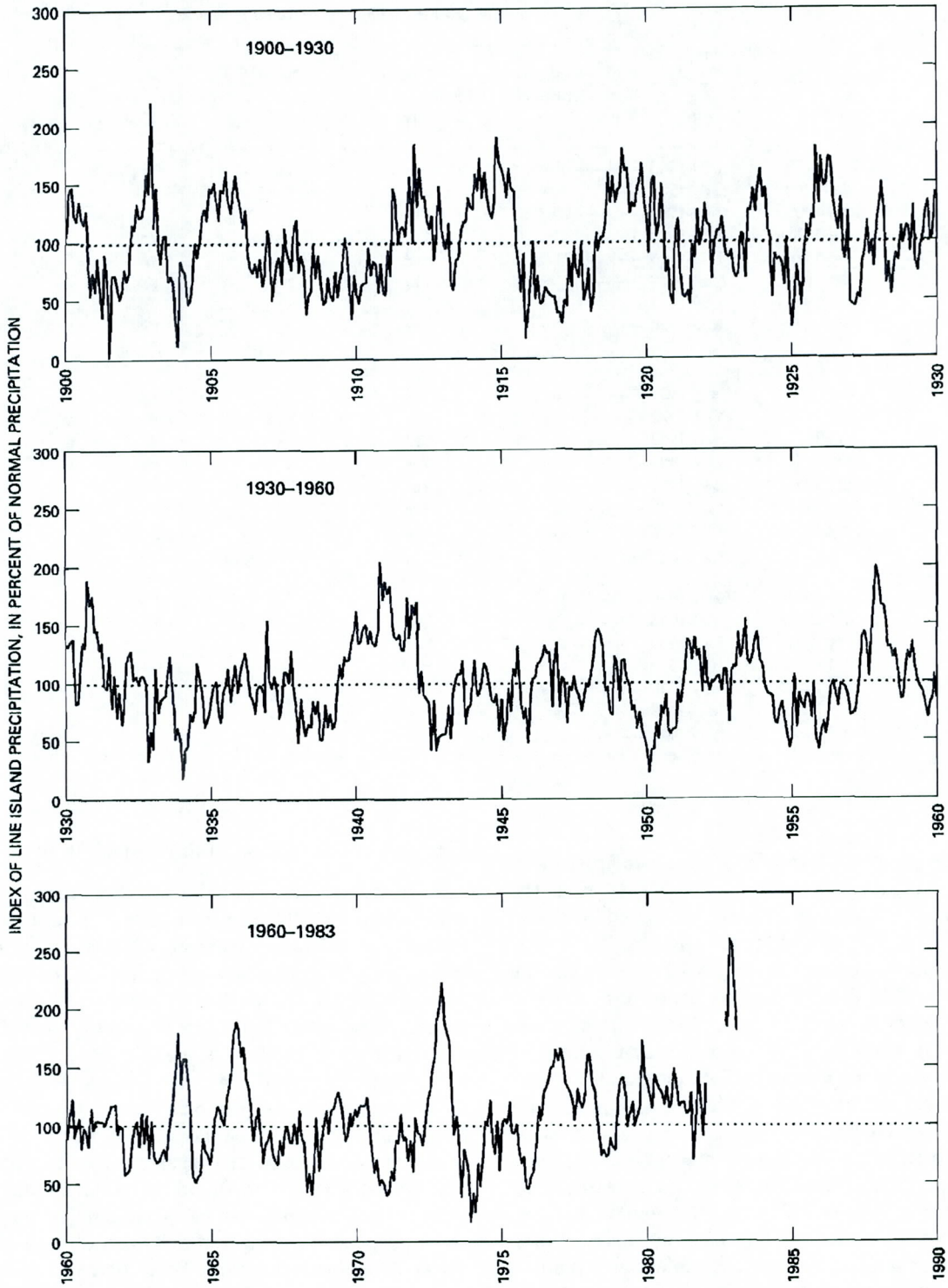

Figure 9. Index of Line Island precipitation (Wright, 1984), representing percent-of-normal precipitation for several stations. Sustained periods with values greater than 100 indicate El Niño-Southern Oscillation conditions.

Table 4. Approximate periods of El Niño-Southern Oscillation conditions in equatorial Pacific Ocean

[Note tendency for El Niño-Southern Oscillation conditions to begin in the early part of the calendar year between 1930 and 1960, compared to midyear before 1930 and after 1960]

Period of time		El Niño-Southern Oscillation conditions agree with			
From	To	Southern Oscillation Index	Line Island Precipitation Index	Quinn and others (1987)	Rasmusson (1984)
Late 1899	Mid-1900	Yes	Yes	Yes	Yes
Mid-1902	Early 1903	Yes	Yes	Yes	Yes
Early 1905	Mid-1906	Yes	Yes	Yes	Yes
Mid-1911	Mid-1912	Yes	Yes	Yes	Yes
Mid-1914	Mid-1915	Yes	Yes	Yes	Yes
Mid-1918	Late 1919	Yes	Yes	Yes	Yes
Mid-1923	Late 1923	Yes	Yes	Yes	Yes
Mid-1925	Mid-1926	Yes	Yes	Yes	Yes
Mid-1930	Early 1931	No	Yes	Yes	Yes
Early 1932	Late 1932	Yes	Yes	Yes	Yes
Mid-1939	Early 1942	Yes	Yes	Yes	Yes
Early 1946	Late 1946	Yes	Yes	No	Yes
Early 1951	Late 1951	Yes	Yes	Yes	Yes
Early 1953	Late 1953	Yes	Yes	Yes	Yes
Early 1957	Mid-1958	Yes	Yes	Yes	Yes
Mid-1963	Early 1964	Yes	Yes	No	Yes
Early 1965	Mid-1966	Yes	Yes	Yes	Yes
Early 1969	Late 1969	Yes	Yes	No	Yes
Mid-1972	Early 1973	Yes	Yes	Yes	Yes
Mid-1976	Early 1978	Yes	Yes	Yes	Yes
Mid-1982	Mid-1983	Yes	Yes	Yes	Yes
Mid-1986	Early 1987	Yes	—	Yes	—

per year were generated during ENSO years compared with 2.3 tropical cyclones per year during non-ENSO years. The annual number of tropical cyclones generated increased from 13.7 for 1965–70 to 16.4 for 1983–88 (fig. 7).

The different recurrences of ENSO during different periods of the 20th century possibly stem from trends in upper-atmospheric pressure over the Northern Hemisphere (Reiter, 1983). Namias (1986) observed that periods of high persistence in the westerly winds precede the Northern Hemisphere mature stage of ENSO by as much as 1 year, which implies that abnormal atmospheric circulation could induce ENSO conditions. Climatic variability on a decadal scale could be driven by long-term increases in the midtropospheric subtropical westerlies and in the frequency of ENSO conditions (Namias and others, 1988). Changes in general atmospheric circulation, therefore, need to be considered in concert with ENSO conditions for an explanation of decadal-scale variability on hydroclimatology in Arizona.

Changes in Circulation of the Upper Atmosphere

In the temperate latitudes, the upper atmosphere generally alternates between two different types of large-scale motion. Zonal flow occurs when winds in the upper atmosphere are predominantly westerly in direction (fig. 5) and usually results in fair weather in Arizona. Meridional flow occurs when winds follow an undulating, wavelike path across the Northern Hemisphere (figs. 4*B*, 5). Meridional flow creates ridges of high pressure and troughs of low pressure that may be stationary for long periods over North America. Meridional flow allows storms to intensify with tropical moisture and penetrate into the Southwest. The spatial distribution of precipitation in the Western United States depends on the axial position, orientation, amplitude, and wavelength of troughs and ridges (Granger, 1984). Meridional flow may break down in transition to zonal flow, and low-pressure eddies in troughs may become separated from the general circulation and become cutoff low-pressure systems (figs. 4*C*, 5; Douglas, 1974).

The long-term frequency of circulation patterns in the Northern Hemisphere has been addressed by Dzerdzeevskii (1969, 1970), Kalnicky (1974), Barry and others (1981), and Carleton (1987). Zonal flow was more common for 1930–60 than before or after (Dzerdzeevskii, 1969; Kalnicky, 1974; Balling and Lawson, 1982). Dzerdzeevskii (1970) classified Northern Hemisphere circulation for each day for 1899–1969 as zonal, meridional, or transitional (fig. 10). The Dzerdzeevskii circulation types shifted to a greater incidence of zonal flow around 1930 and back to a dominance by meridional flow beginning in the 1950's (fig. 10; Dzerdzeevskii, 1969). The greater incidence of meridional flow in the latter part of the series has continued into the 1980's (Balling and Lawson, 1982).

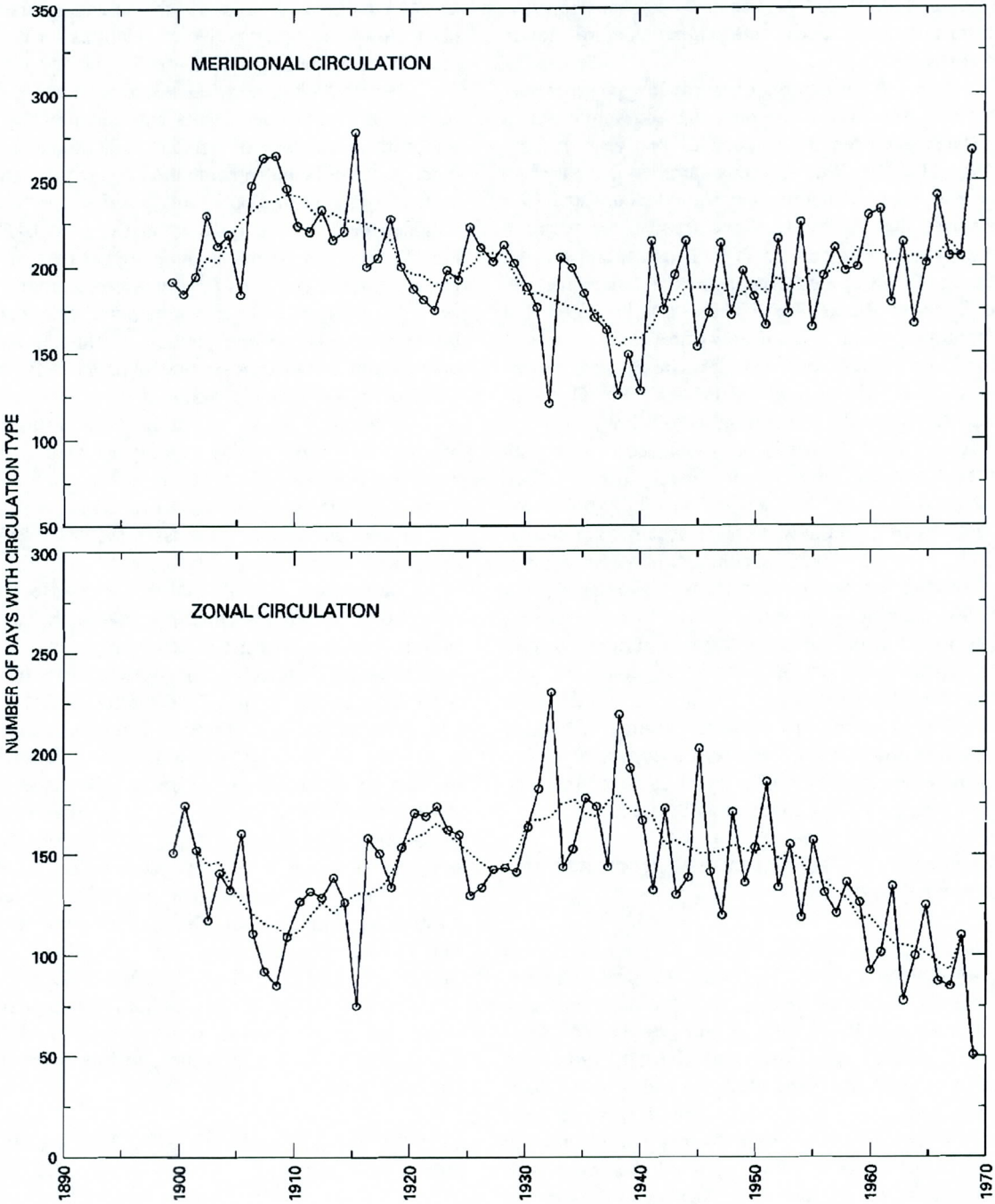

Figure 10. Time series of meridional and zonal flow in upper atmosphere from 1899 to 1970 (Dzerdzeevskii, 1970). Dotted lines represent the 6-year running mean.

The temporal incidence of cutoff low-pressure systems suggests another measure of fluctuations in general circulation. As noted previously, cutoff low-pressure systems evolve during the breakdown of meridional flow in the upper atmosphere. Generally, a low-pressure cell is present near latitude 55° N. and longitude 140° W., and low-pressure eddies move eastward from that area to produce precipitation across the United States. During meridional flow, some low-pressure eddies move as far southward as latitude 25° N. become detached from the westerly circulation pattern, and stagnate before slowly drifting eastward.

For 1945–59, the number of cutoff low-pressure systems that occurred over the continental and southwestern United States averaged 31.9 and 21.3 per year, respectively (fig. 11). For 1960–88, this number decreased to 29.3 per year over the continental United States and 19.2 per year over the Southwest. Concurrently, the variance decreased by about 60 percent in both cases, and the decrease is significant at the 95-percent confidence level using the Squared Ranks Test. These results suggest a greater continuity of meridional flow after 1960.

The incidence of cutoff low-pressure systems in certain months is significantly correlated with ENSO conditions. For example, the number of cutoff lows over the Southwestern United States is negatively correlated with the sea-level pressure difference in January ($r = -0.460$), March ($r = -0.316$), and November ($r = -0.474$). The average numbers of cutoff low-pressure systems are similar during ENSO and non-ENSO conditions; however, seasonally, the average numbers of cutoff lows increases slightly under ENSO conditions for the months of March, October, and November. For example, the average numbers of cutoff lows during March are 3.15 for ENSO conditions and 2.32 for non-ENSO conditions. The joint occurrence of a slight increase of cutoff low-pressure systems in the fall with a slightly increased generation of tropical cyclones suggests increased incidence of tropical cyclones that dissipate over Arizona during ENSO conditions.

El Niño-Southern Oscillation and Precipitation in Southern Arizona

Climate in southern Arizona is teleconnected with the equatorial Pacific Ocean. For example, correlations between SOI and seasonal precipitation for many Arizona stations are statistically significant and negative (Andrade and Sellers, 1988; Ropelewski and Halpert, 1986; and Douglas and Englehart, 1984). Andrade and Sellers (1988) found that precipitation in Arizona and western New Mexico is enhanced in the normally dry spring and fall during ENSO conditions. They suggested that warm sea-surface temperatures off the west coasts of Mexico and California (1) provide the necessary energy for the development of strong west coast troughs, (2) weaken the tradewind inversion and thus allow moist air to penetrate into the Southwest, and (3) cause stronger, more numerous Pacific tropical cyclones than usual. Douglas and Englehart (1984) found significant positive correlations between the index of Line Island summer precipitation and precipitation in the southwestern United States during October, November, and the following February and March (fig. 12). These months are also ones in which the incidence of cutoff low-pressure systems increased under ENSO conditions. Southern Arizona and southern California yield the highest positive correlations for each of these months for latitudes south of 40° N. (fig. 12).

For 1900–82, seasonal teleconnections are reflected in the correlation coefficients between monthly precipitation at the University of Arizona at Tucson station and the index of Line Island precipitation for the current and previous (lag 1) year. Significant positive correlations were obtained between precipitation in the Line Islands for all months from the previous June to the current April and precipitation at the University of Arizona from February to May (table 5). Significant correlations were also obtained between Line Island precipitation in summer and fall with precipitation at the University of Arizona between October and November (table 5). Some of these correlations imply a 4- to 6-month lag in the midlatitude atmosphere-ocean response to processes that occur at the equator. Significant relations between precipitation in the Line Islands and Tucson for the same month, however, suggest a more direct link to tropical cloud masses moving northeast from the central equatorial Pacific Ocean.

Betancourt (1990) analyzed the effect of ENSO conditions on Tucson precipitation using a 36-month period centered on June of an average year with ENSO conditions. Precipitation is significantly increased in most months during and 1 year after ENSO conditions; precipitation for April through June and October is significantly higher than for non-ENSO conditions. Significantly reduced precipitation in August, during ENSO conditions, indicates a suppression of summer monsoonal precipitation under ENSO conditions. Sellers (1960) found a negative correlation between September and July and August precipitation for 1898 to 1959 in Arizona. Under ENSO conditions, precipitation begins earlier in fall months in the southwestern United States (Kiladis and Diaz, 1989). Sellers (1960) and Betancourt (1990) suggested that atmospheric conditions that are conducive to monsoonal precipitation are somewhat exclusive of precipitation from dissipating tropical cyclones.

Hydrologic Variability in the Santa Cruz River Basin

Various indices and proxy records indicate shifts in climate around 1930 and 1960. Because Arizona's climate

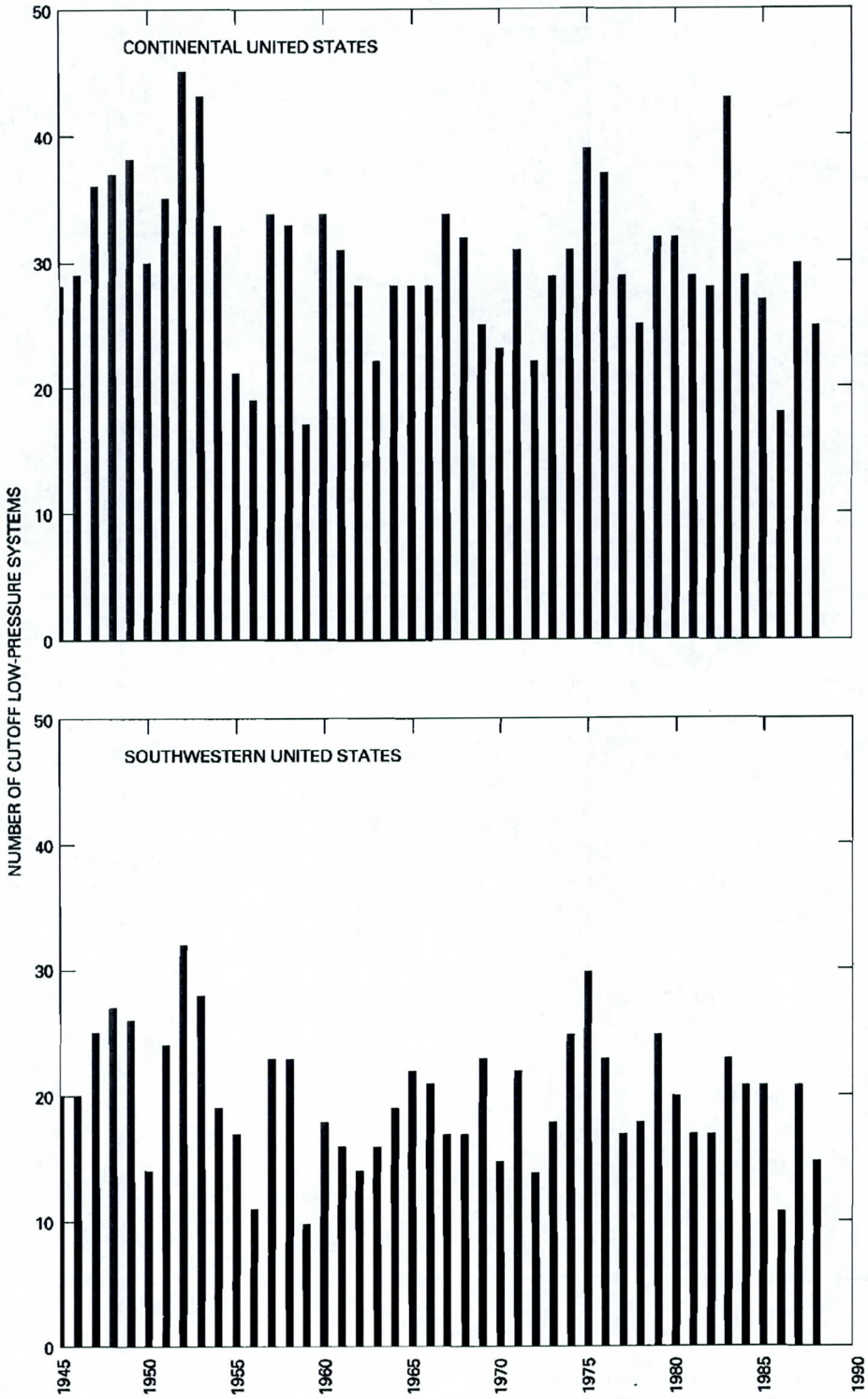

Figure 11. Annual frequency of cutoff low-pressure systems, which are defined as 2 days with one closed geopotential height on a 500-millibar height map (National Oceanic and Atmospheric Administration, 1988). Cutoff low-pressure systems occur over the Continental United States between lat 20° N. and 45° N. and long 65° W. and 140° W. and in the Southwestern United States between lat 20° N. and 45° N. and long 100° W. and 140° W.

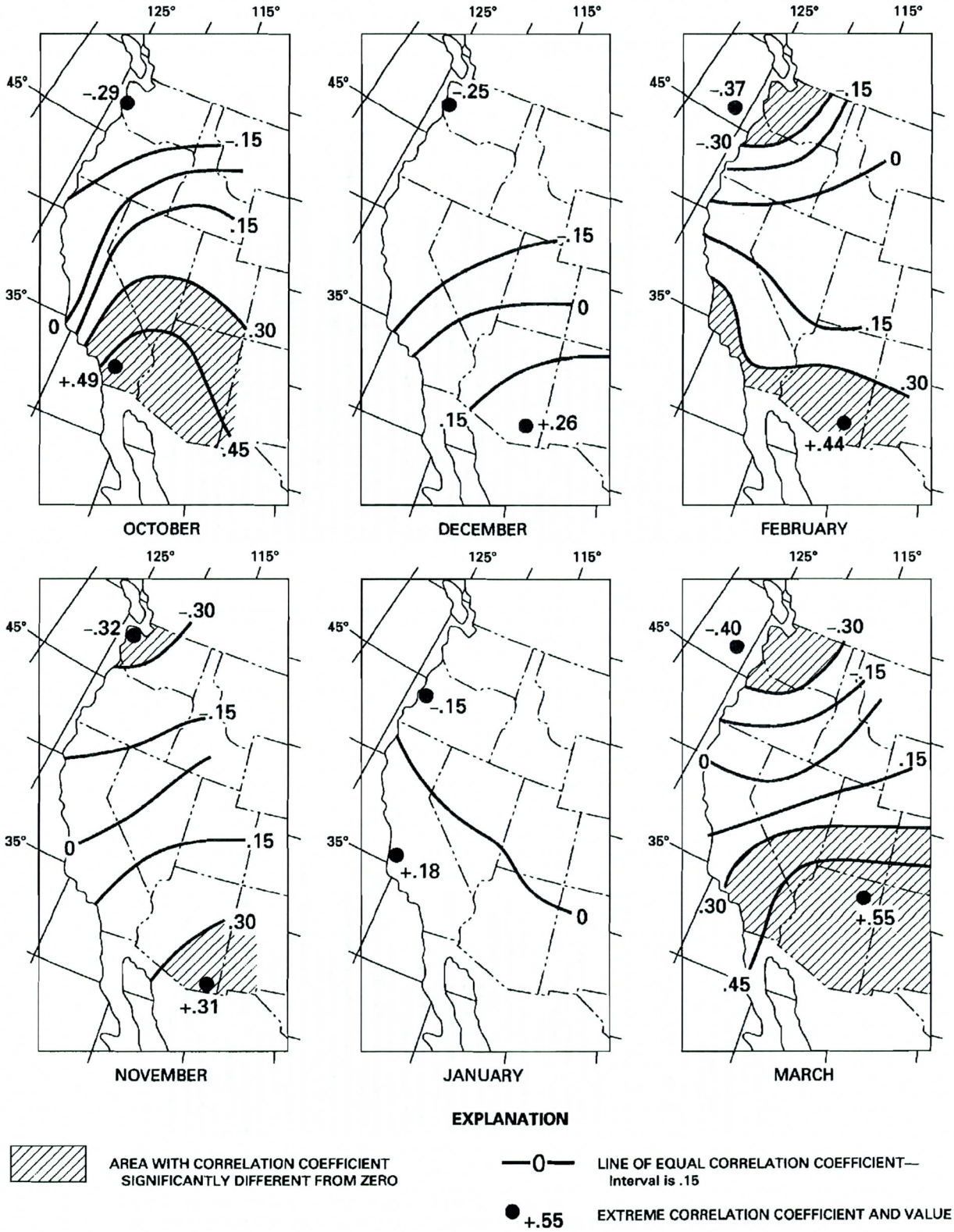

Figure 12. Correlations between the index of Line Island precipitation for the equatorial Pacific Ocean and precipitation in the Western United States (Douglas and Englehart, 1984).

Table 5. Matrix of correlation coefficients between Line Island monthly precipitation and Tucson monthly precipitation, 1900–82

[Comparison begins with Line Island precipitation in June of the previous year to check for lag effects on Tucson precipitation. Pearson correlation coefficients greater than or equal to 0.22 are significantly different from zero at the 95-percent confidence level. Significant values are underscored. Note that correlation coefficients greater than 0.28 are significantly different from zero at a 99-percent confidence level]

Tucson precipitation	Index of Line Island precipitation																	
	June	July	Aug.	Sept.	Oct.	Nov.	Dec.	Jan.	Feb.	Mar.	Apr.	May	June	July	Aug.	Sept.	Oct.	Nov.	Dec.
Jan.	-0.11	-0.15	-0.13	0.03	-0.09	-0.08	-0.02	-0.01	-0.03	0.07	0.01	-0.05	0.04	0.02	-0.14	-0.03	0.02	-0.06	-0.02
Feb.	.22	.27	.26	.37	.34	.43	.33	.36	.27	.19	.21	.08	.12	-.01	.05	.08	.05	.03	.16
Mar.	.25	.28	.47	.42	.45	.47	.51	.38	.41	.31	.24	.19	.15	.04	-.07	.05	.00	.01	-.01
Apr.	.14	.16	.27	.27	.26	.20	.31	.33	.25	.24	.28	.21	.28	.14	.26	.19	.12	-.08	.10
May	.02	.11	.17	.14	.16	.22	.25	.17	.19	.22	.24	.11	.23	.06	.13	.29	.25	.18	.23
June	.02	.12	.12	.19	.14	.06	.09	.05	.06	.07	.00	-.01	.06	.06	.12	.11	.16	.14	.14
July	-.05	-.06	-.15	-.16	-.17	-.19	-.10	-.10	-.09	-.14	-.12	-.26	-.28	-.17	-.19	-.10	-.16	-.19	-.22
Aug.	-.01	.00	-.10	-.15	-.11	-.15	-.14	-.08	-.10	-.13	.10	-.15	.08	.05	-.07	-.06	.05	.05	.09
Sept.	.06	-.13	.08	.12	.14	.05	.04	.02	.03	.05	.14	.09	.12	.23	.18	.01	.06	.10	.16
Oct.	.00	-.17	.03	-.06	.06	-.13	.06	.03	.04	.14	.23	.30	.22	.34	.21	.21	.30	.29	.29
Nov.	-.01	-.20	.22	.16	.17	.13	.19	.17	.20	.17	.17	.13	.33	.25	.37	.29	.34	.27	.24
Dec.	.02	.04	.06	-.06	.10	.04	.08	.09	.11	.15	.15	.08	.16	.11	.15	.19	.20	.24	.07

is linked with these climatic processes, some differences in climatic and hydrologic regimes would be expected for different periods of the 20th century. The periods of 1900–29, 1930–59, and 1960–86 were chosen for comparison because they represent approximately equal numbers of years. The intensity and amount of precipitation at the University of Arizona at Tucson station changed after 1960. Extreme precipitation events of 1- to 7-day duration increased significantly after 1954 for September to October and January to February (Kenneth Young, University of Arizona, written commun., 1985). Likewise, the frequency of days with more than 25 mm of rainfall during the summer months increased significantly in the 1950's (Betancourt, 1990). Heavy rains were also frequent in the late 1800's, when large floods initiated the arroyo that now marks the course of the Santa Cruz River.

Streamflow in the Santa Cruz River also has changed during the 20th century. The seasonality of annual floods changed after about 1960 (fig. 2). The amount of seasonal runoff, in accordance with the annual flood series, varies significantly during the 20th century. Seasonal cumulative departures from mean streamflow (fig. 13) indicate that below-average runoff occurred during 1920–60 in winter and fall. Streamflow in winter and fall increased episodically in the mid-1960's, late 1970's, and early 1980's (fig. 13). The graphs in figure 13 reflect changes in the annual flood series (fig. 2). Conversely, summer runoff increased from 1949 to the late 1950's and then steadily decreased until 1985.

Duration analyses of daily streamflow at the gaging station, Santa Cruz River at Tucson, reveal marked changes with time. Daily discharges in summer months that were exceeded less than 2 percent of days were much higher for 1930–59 than for 1915–29 or for 1960–81 (fig. 14). Conversely, daily discharges in fall months that were exceeded less than 2 percent of days were much less for 1930–59 than before or after. Cumulative-departure curve patterns and duration-analysis results reflect the enhancement of fall and winter precipitation and the suppression of summer precipitation during periods of increased frequency of ENSO conditions before 1930 and after 1960.

FREQUENCY ANALYSIS OF ANNUAL FLOODS IN THE SANTA CRUZ RIVER

Previous Estimates of the 100-Year Flood

The flood of October 1983 on the Santa Cruz River heightened public awareness of flood-frequency estimates. Even before the flood of October 1983, estimates of the 100-year flood for the Santa Cruz River at Tucson were controversial (Michael Zeller, Simons Li and Associates, written commun., 1984). Knapp (1937) first estimated the 100-year flood to be 355 m^3/s from a record length of 20

years. Schwalen (1942) estimated the 100-year flood to be 450 m^3/s from a record length of 27 years. Recent estimates range from 572 to 2,780 m^3/s (table 2) and were derived by applying different methods and assumptions to varying lengths of record both before and after the 1983 flood (table 2).

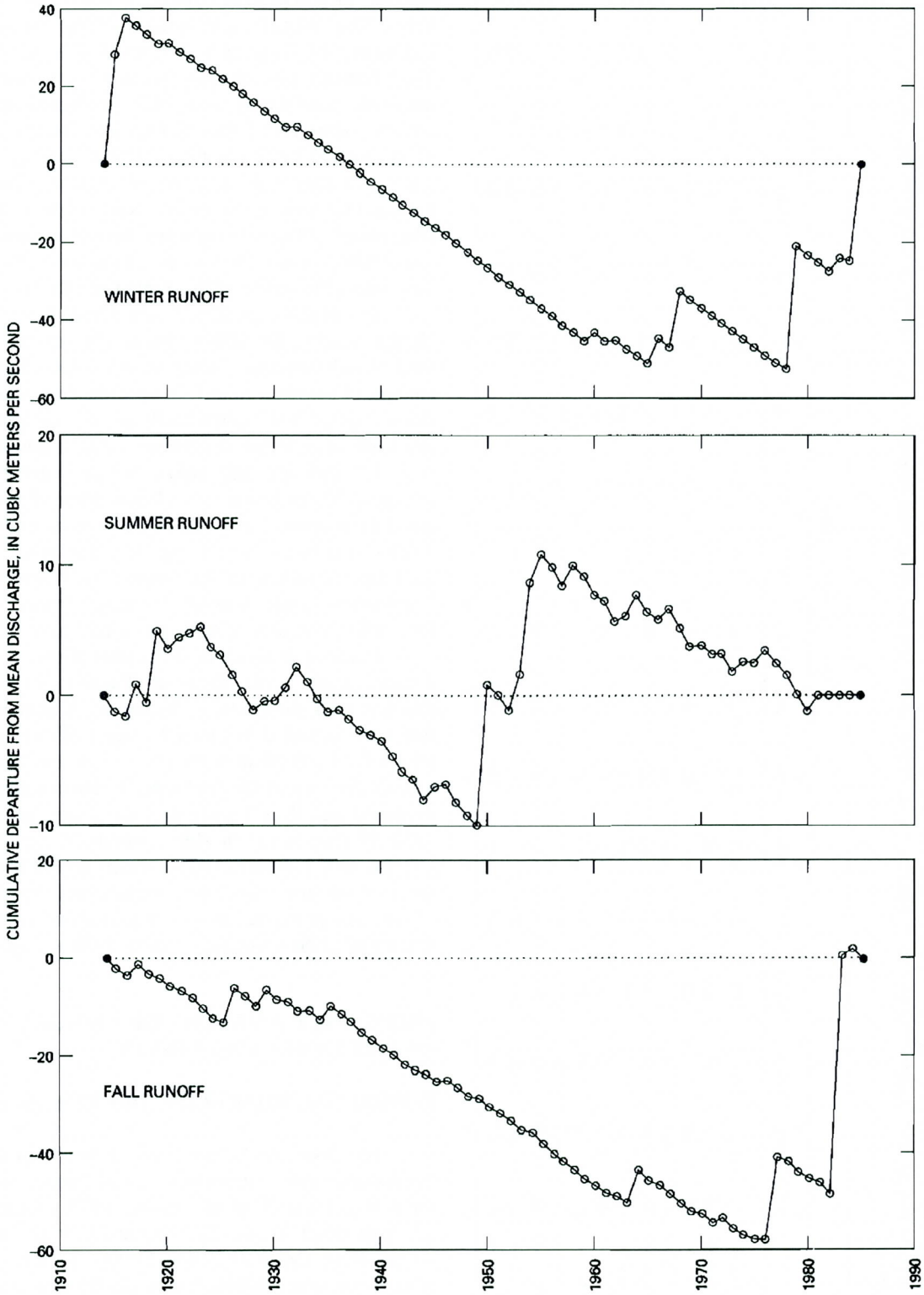

Figure 13. Seasonal cumulative departures from mean discharge, Santa Cruz River at Tucson, Arizona.

After the flood of 1983, local authorities reacted to discrepancies in the 100-year flood estimates by commissioning studies and amending existing flood-plain legislation. A deterministic hydrologic simulation model using 100-year-frequency rainfall of 24-hour, 48-hour, and 96-hour durations was used in one study (Ponce and others, 1985). The model was calibrated by hindcasting the runoff hydrograph of the flood of October 1983.

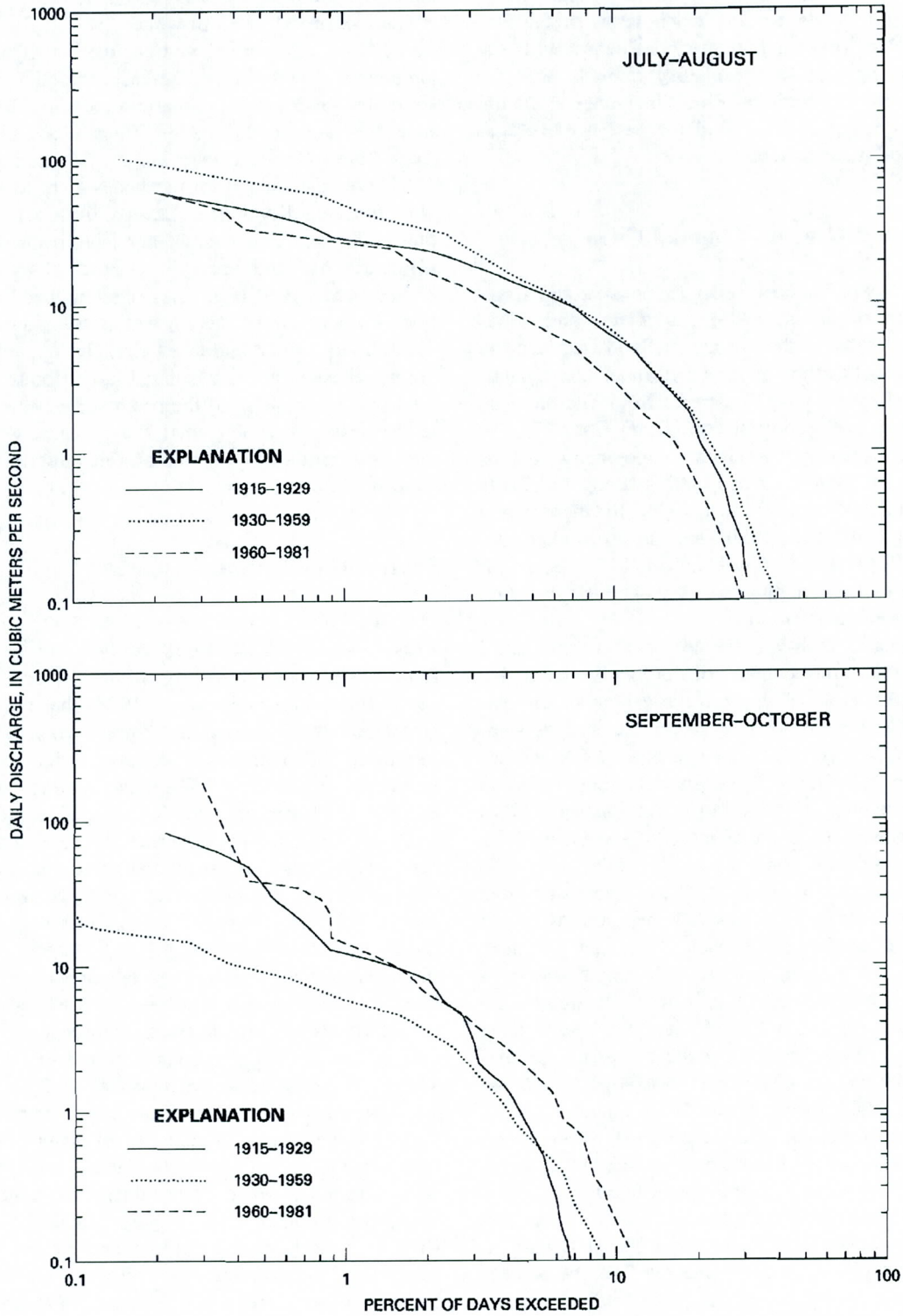

Figure 14. Duration analyses of daily discharge for two periods, Santa Cruz River at Tucson, Arizona.

Some of the assumptions relating to tributary inflow during the flood of October 1983 have been questioned (Hjalmarson, 1987). On the basis of the rainfall-runoff model, both Pima County and the city of Tucson adopted a "regulatory flood" of 1,700 m^3/s and a "design flood" of 1,980 m^3/s in 1985 for the reach between the San Xavier del Bac Mission and the confluence with the Rillito River (fig. 1). The regulatory flood is used for compliance with the National Flood Insurance Program, whereas the design flood is used for design of bridges and other flood-plain structures.

Effects of Land Use and Channel Change

Reich (1984), Michael Zeller (Simons Li and Associates, written commun., 1984), and Reich and Davis (1985, 1986) attributed the change in flood frequency to increased channelization, improved channel conveyance, and reduced channel storage upstream from Tucson since establishment of the gaging station, Santa Cruz River at Tucson, in 1915. Changes in channel topography, such as those that evolved from arroyo-cutting along the Santa Cruz River (Cooke and Reeves, 1976; Betancourt and Turner, 1988; Betancourt, 1990), are known to alter conveyance of flood waves (Burkham, 1981). The result would be an increase in the peak discharge downstream for the same volume of runoff.

The Santa Cruz River did not have an entrenched channel near the south boundary of the San Xavier Indian Reservation (fig. 1) in 1915, when the gaging station was established at Tucson. In the reservation, the channel deepened 3 to 5 m between 1915 and the late 1930's and another 2 to 3 m since then. The channel bottom at Tucson incised 3 to 5 m after 1946 (Aldridge and Eychaner, 1984) apparently because of encroachment of the channel by landfills and highway construction. Hypothetically, the flood in December 1914, which produced a peak discharge of 425 m^3/s, would yield a much higher peak if routed through the modern incised channel. Conversely, the peak discharge of 1,490 m^3/s in October 1983 might have been much less if it had flowed through the discontinuous arroyo system that existed in 1915. Preliminary results using a flow-routing model, however, yielded only an approximate 15- to 20-percent decrease in discharge by routing the flood of 1983 through the 1915 channel (H.W. Hjalmarson, hydrologist, U.S. Geological Survey, oral commun., 1989). Local channel erosion, therefore, is not the sole reason for changes in the annual flood series.

Annual floods have increased in size at all gaging stations on the Santa Cruz River (fig. 15). At Lochiel, a flood in August 1984 was larger than the flood of October 1983 (fig. 15*A*). No significant change in land use has occurred upstream from the gaging station at Lochiel. At Nogales (fig. 15*B*), where land use in Mexico could have altered flow conveyance, five of the six largest floods occurred between 1968 and 1983. The annual flood series for other gaging stations on the Santa Cruz River also show an increase in annual peaks (fig. 15*C*, *E*, *F*). At Tucson, six of the seven largest floods occurred after 1960 and five of these occurred in fall or winter (table 1; fig. 15*D*).

Although land use and changes in channel conveyance undoubtedly have increased flood discharges to some unknown extent, climatic effects are the only common link among the six gaging stations on the Santa Cruz River. Only the very largest floods, as in October 1983, are sustained from the headwaters to the juncture with the Gila River near Laveen. At Lochiel, flows in the Santa Cruz River could not have been affected significantly by land use, yet peak discharges have increased since 1960 (fig. 15*A*). The August 1984 flood at Lochiel, the peak of record, was larger than the October 1983 flood, which indicates that the apparent changes are not caused by a few isolated large floods. Changes in the hydroclimatology of the basin are reflected by a shift in the seasonality of annual flood peaks, which is also the most striking symptom of the underlying climatic control of flood frequency.

Seasonality of Annual Floods

The annual flood series of the Santa Cruz River at Tucson shows a lack of uniformity in the seasonality of flood peaks (table 1, fig. 2; Keith, 1981; Hirschboeck, 1985; Betancourt and Turner, 1988) that may partly account for the increase in annual peaks since 1960. Floods in July and August accounted for 75 percent of the annual peaks for 1915–86, and summer had the largest and least-variable monthly discharges (fig. 3). For 1915–29 and 1960–86, however, 53 percent and 39 percent, respectively, of the annual flood peaks occurred in fall (September to October) or winter (November to February). For 1930–59, only 3 percent of the peaks occurred in fall or winter. Seven of the eight largest peaks in the flood series were produced by fall or winter storms, and five of these occurred in 1960–86. Whereas most of the annual floods at Nogales occurred in summer (fig. 15*B*), four of the six largest floods occurred in fall or winter. These changes indicate that seasonality of flooding is not stationary or random on the Santa Cruz River.

The change in seasonality of annual flood peaks after 1960 is not unique to the Santa Cruz River but also occurs on other streams in southern and central Arizona that have drainage areas larger than about 2,000 km^2. Rillito Creek (Slezak-Pearthree and Baker, 1987), San Francisco River (Hjalmarson, 1990), and the Gila and San Pedro Rivers (Roeske and others, 1989) are some examples. The largest floods on these rivers commonly occur in fall and winter, although annual peaks also occur in

summer. The storm types that are responsible for these floods are dissipating tropical cyclones, cutoff low-pressure systems, and frontal systems.

The change in seasonality of annual floods indicates low-frequency climatic variability as the principal reason for increased flood frequency on the Santa Cruz River. Al-

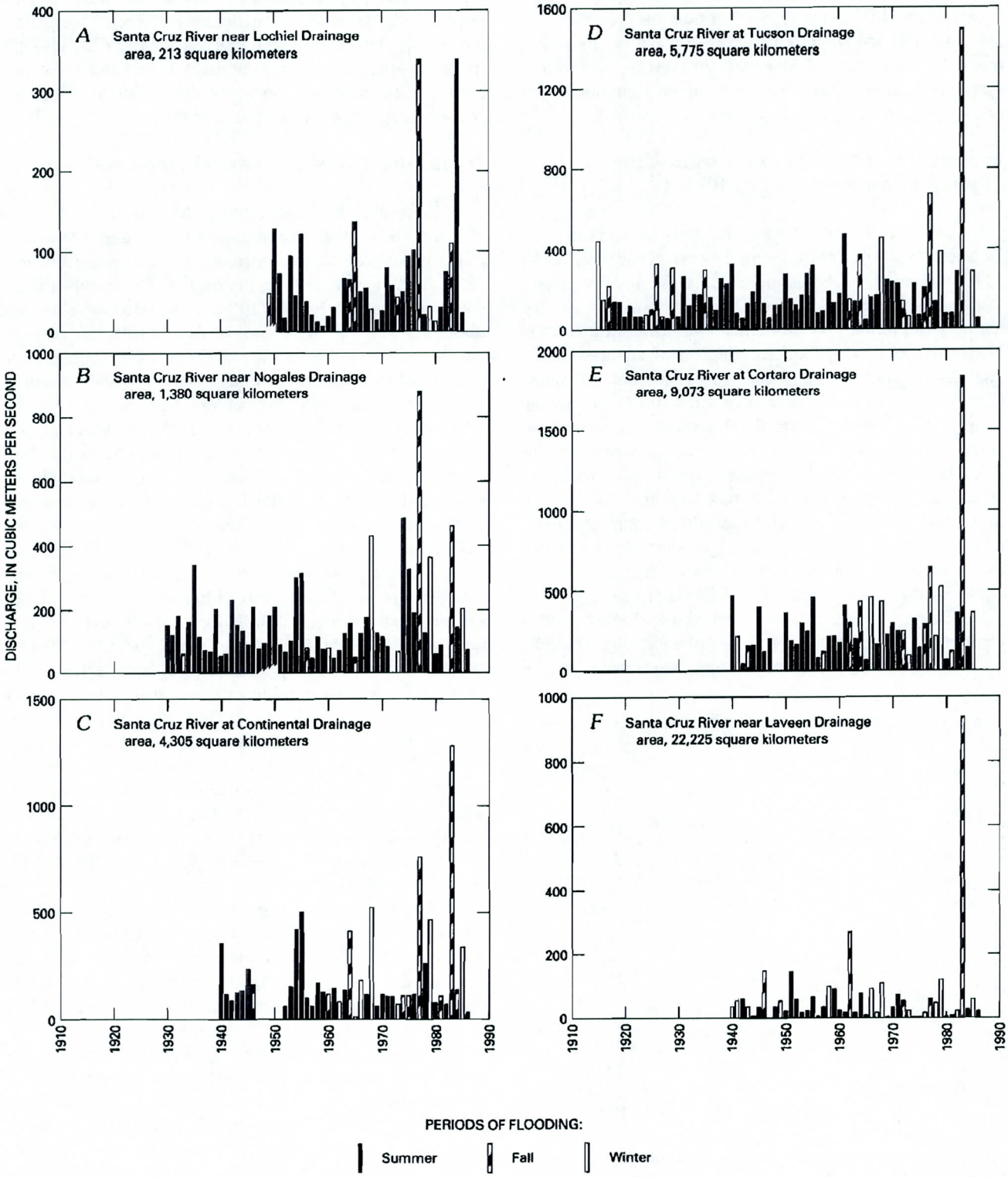

Figure 15. Annual flood series for six gaging stations, Santa Cruz River, southern Arizona. Hydroclimatological year, November 1 to October 31.

though land-use practices may have produced a modest increase in discharges, climatic variability is the only possible reason for changes in the seasonality of flooding. As will be shown, the best explanation for the change in seasonality is a shift in the type of storms that cause floods. Storms in fall and winter after 1960—related to dissipating tropical cyclones, cutoff low-pressure systems, and frontal systems—caused floods that were larger than floods between 1930 and 1959.

Estimates of 100-Year Discharges Using Method of Moments, 1970–85

The stability of 100-year flood estimates is one indication of stationarity in an annual flood series. In 1970, the length of the annual flood series for the gaging station, Santa Cruz River at Tucson, was 55 years. By using the method of moments and assuming a log-Pearson type III distribution, addition of successive annual floods after 1970 affected 100-year flood estimates (fig. 16; Interagency Advisory Committee on Water Data, 1982). The 100-year flood estimates increased 16 percent or 90 m^3/s for 1970–82. The influence of the flood of October 1983 is apparent in the 50-percent increase in 100-year flood estimates—from 577 to 872 m^3/s—for 1971–86. The 100-year flood estimated from annual peaks for 1915–86 is larger than the band between the 10- and 90-percent confidence intervals for the value estimated from peaks for 1915–71 (fig. 16).

Changes in the standard deviation and skew coefficient of the log-Pearson type III distribution (fig. 17) indicate the statistical cause for changes in estimates of the

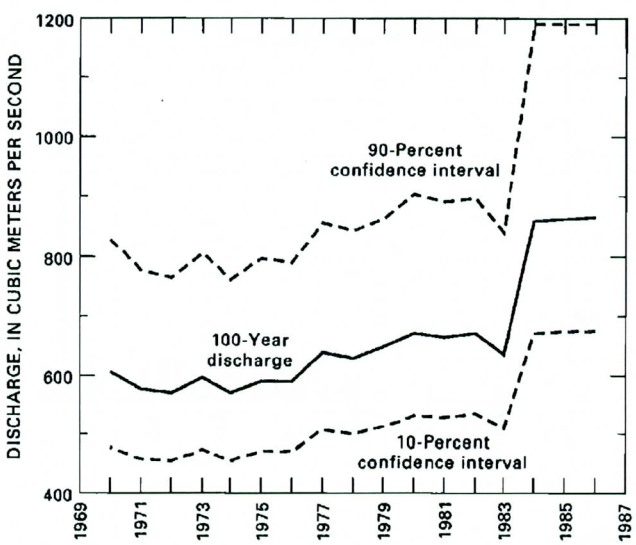

Figure 16. Chronology of 100-year flood estimates for the Santa Cruz River at Tucson, Arizona, 1970–86. The skew coefficient is weighted using a generalized skew coefficient of –0.2 with a mean-squared error of 0.302.

100-year flood. Although the mean and variance do not change significantly with addition of successive annual floods, the skew coefficient increases from –0.29 to 0.30 for 1971–86 (fig. 17) because of the preponderance of large floods. Despite the moderating effect of weighting the sample skew coefficient with a generalized skew coefficient of –0.2 (Interagency Advisory Committee on Water Data, 1982), the larger skew coefficient underlies the increase in discharge for the 100-year flood.

Trend Analysis of the Annual Flood Series

According to Reich (1984), the annual flood series changed about 1960 to a regime of increased flood size. Using a Kruskal-Wallis nonparametric test (see Conover, 1971, p. 229) on data from the gaging station, Santa Cruz River at Tucson, Reich (1984) concluded that annual floods for 1915–59 were derived from a different population than annual floods for 1960–84. H.W. Hjalmarson (U.S. Geological Survey, written commun., 1985) detected a positive trend in the annual flood series for 1915–84 using Pearson product-moment correlation analysis and moderate trends using other nonparametric tests. The Pearson product-moment correlation results were highly influenced by the 1983 flood, whereas the nonparametric tests were not. Hjalmarson's results also suggest that annual floods were larger after 1960.

Although the means for 1915–29, 1930–59, and 1960–86 are not significantly different, the mean of the annual flood series is 147 m^3/s for 1915–29 and 267 m^3/s for 1960–86 (table 6). The variances for 1915–29 and 1930–59 are significantly less than the variance for 1960–86 at a 95-percent confidence level using the Squared Ranks Test (Conover, 1971). These results suggest that the annual flood series at Tucson may result from weak stationarity of order 1—the mean is time invariant although the variance and skew coefficient change with time (Box and Jenkins, 1971, p. 30). The annual flood series at Cortaro yields similar results because the correlation coefficient between the two series is 0.938 (r = 0.785 without the flood of 1983).

Trend analysis was performed on the annual flood series using two nonparametric tests. Kendall's tau-b (Conover, 1971) and Spearman rank-correlation analyses were used to detect any significant trends in the annual flood series and (or) segments of the flood series. Most of the analyses did not yield significant trends at the 95-percent confidence level (table 6). Kendall's tau-b analyses indicate no significant trends in or between any of the periods. Using the Spearman rank correlation, only floods for 1915–29 had a significantly negative trend (table 6). Lack of significant trends for most periods could be explained by a lack of significant differences among the mean annual floods of the various periods, which trend analysis is designed to detect. Changes in

the variance and skew apparently are not large enough to yield significant trends in or between the periods. The absence of significant trends within periods suggests that, with the possible exception of 1915–29, each of the three segments of the annual flood series may have arisen from a homogeneous population.

Flood Frequency During El Niño-Southern Oscillation Conditions

The annual flood series of the Santa Cruz River is also affected by ENSO conditions. Four of the five largest and six of the ten smallest annual floods at Tucson occurred during ENSO conditions. For ENSO conditions, the mean discharge and standard deviation for 27 annual floods at Tucson are 226 and 288 m^3/s. For non-ENSO conditions, the mean and standard deviation for 44 annual floods are 181 and 111 m^3/s. The means of the respective series are not significantly different, but the variance during ENSO years is significantly increased. Using the nonparametric Squared Ranks Test statistic (Conover, 1971, p. 239–240), the variance for ENSO years is significantly greater than that for non-ENSO years at the 95-percent confidence level.

Flood frequency was estimated using procedures given in Interagency Advisory Committee on Water Data (1982) for ENSO and non-ENSO years (fig. 18). A tenuous assumption of stationarity over the period of record is required for the frequency analysis. A generalized skew coefficient of –0.2 was used to weight the station skew. The estimated 100-year floods for ENSO and non-ENSO years are 1,300 and 628 m^3/s, respectively, at Tucson (table 7). The frequency relations begin to diverge substantially above about a 25-year recurrence interval (fig. 18). At Cortaro, the estimated 100-year floods for ENSO and

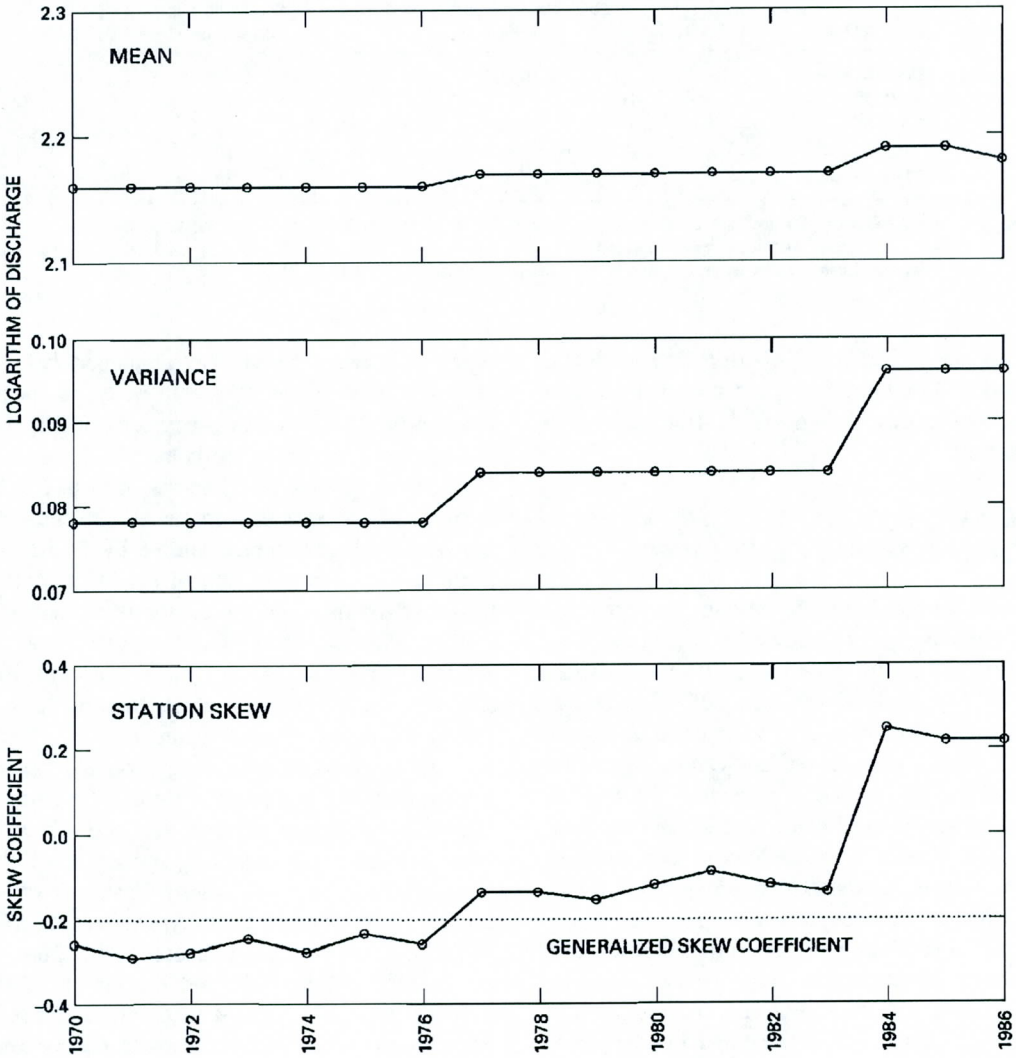

Figure 17. Chronology of moments of the log-transformed annual flood series of the Santa Cruz River at Tucson, Arizona, 1970–86. Values were estimated using U.S. Water Resources Council (1981) methods and a generalized skew coefficient of –0.2 with a mean-squared error of 0.302.

Table 6. Statistical properties and trend-analysis results for five periods of the annual flood series, Santa Cruz River at Tucson, Arizona

Period	Number of years	Mean discharge, in cubic meters per second	Standard deviation, in cubic meters per second	Mean logarithm of discharge	Standard deviation of log discharge
All	71	199	198	2.17	0.319
1915–29	15	147	117	2.05	.321
1930–59	30	166	85	2.16	.248
1960–86	26	267	292	2.27	.371
ENSO years	27	226	288	2.18	.368
Non-ENSO years	44	181	111	2.17	.288

Period	Kendall's tau-b		Spearman rank correlation	
	Tau-b	Probability of significance[1]		Probability of significance[1]
1915–29	–0.36	0.067	–0.64	[2]0.014
1930–59	–.01	.96	–.051	.79
1960–86	–.01	.98	.019	.98
1915–86	.13	.12	.19	.12
1930–86	.09	.34	.12	.38

[1]Probability of significance refers to the probability level at which the null hypothesis of no significant slope can be rejected.
[2]A significant trend was determined at the 95-percent confidence level.

non-ENSO years are 1,620 and 746 m^3/s, respectively. Whether or not ENSO conditions occur has an important effect on flood frequency regardless of fluctuations in 20th-century climate.

HYDROCLIMATIC FLOOD-FREQUENCY ANALYSIS OF THE SANTA CRUZ RIVER

Analyses of oceanic and atmospheric processes that lead to storms and subsequent flooding in Arizona suggest that the 20th century has at least three distinct hydroclimatic periods—1900–29, 1930–59, and 1960–86. Transitions between these periods appear to be gradational instead of abrupt. The increased frequency of ENSO conditions after 1960 has apparently enhanced the generation of tropical cyclones in the eastern North Pacific Ocean, and the relation of increased incidence of cutoff low-pressure systems with ENSO conditions suggests an increased probability for recurvature of tropical cyclones into North America. Frontal storms are enhanced by an increase in meridional circulation, a deepened Aleutian low, and greater moisture availability from the North Pacific Ocean. The duration of the period that began about 1960 is unknown, but the period appears to have been stable until at least 1986.

These results pose a challenge for statistical flood-frequency analysis of rivers in Arizona. Certain storm types that cause floods are enhanced before 1930 and after 1960, whereas other storm types may occur less frequently. The low-frequency temporal shifts in hydroclimatology support the empirical observation that changes in annual flood series are caused by temporal changes in variance and (or) skew coefficient, instead of the mean. Larger floods caused by frontal systems and tropical cyclones could be offset by a decrease in incidence of the more common floods caused by monsoonal storms. This possible offset suggests that annual flood series, such as the one for the Santa Cruz River at Tucson (fig. 2), are weakly stationary and have a changing variance and (or) skew coefficient.

One means of estimating annual flood frequency for a river such as the Santa Cruz might be to consider floods caused by different storm types as independent populations. Although the sampling properties of these populations probably are continuous functions of time, floods caused by different storm types may be stationary for 1930–60 and 1960–86. Because no partial-duration series is available before 1930 and the length of the period is only 15 years, this period was not considered separately. Samples from the separate periods can be fitted to probability distributions with different assumptions concerning the expected effects of the shifts in oceanic and atmospheric processes on their statistical properties. The

separate populations can then be combined using mixed-population analysis to estimate annual flood-recurrence intervals.

Separation of Floods by Storm Types

Hirschboeck (1985) analyzed the hydroclimatology of floods for 1950–80 in the Gila River basin of which the Santa Cruz River basin is a part. She identified populations of floods caused by snowmelt and eight types of storms and classified all floods for 30 gaging-station records, including Santa Cruz River at Tucson and Santa Cruz River at Cortaro, in the partial-duration series. Storm types were identified using various data sources including daily weather maps (National Oceanic and Atmospheric Administration, 1988), 700- and 500-millibar heights, tropical cyclone reports, and precipitation data (Hirschboeck, 1985).

Hirschboeck's (1985) classification scheme cannot be applied to floods before 1945 because of the absence of 700- and 500-millibar height data. To obtain consis-

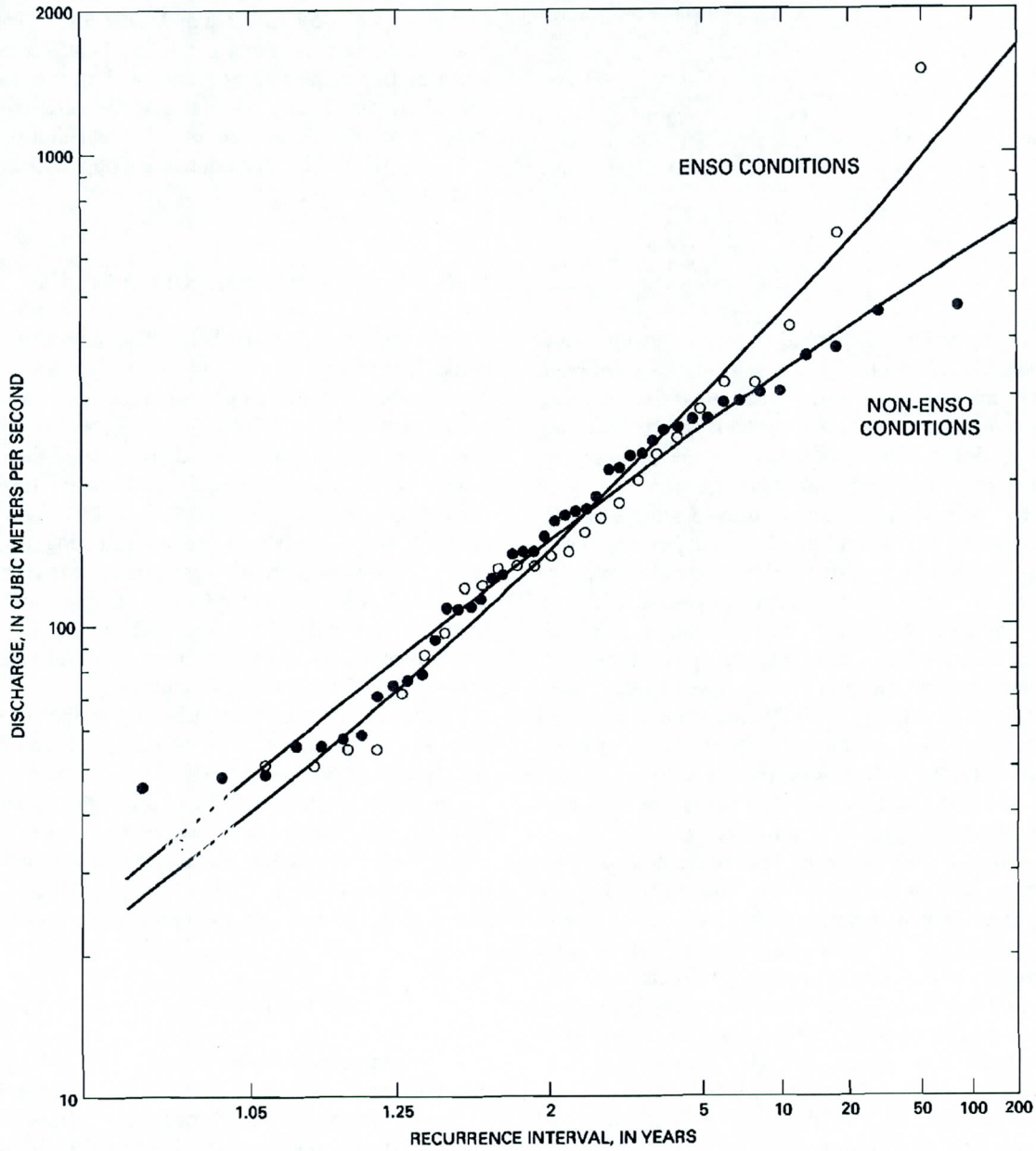

Figure 18. Flood frequency for years with and without El Niño-Southern Oscillation conditions, Santa Cruz River at Tucson, Arizona. The skew coefficient is weighted using a generalized skew coefficient of –0.2, with a mean-squared error of 0.302.

Table 7. Estimates of the 100-year flood for the Santa Cruz River calculated using different methods and based on different assumptions

[Methods: MM, procedures specified in Interagency Advisory Committee on Water Resources (1982) and a generalized skew coefficient of –0.2; ML, maximum-likelihood analysis of type I censored data (Stedinger and others, 1988); MP, mixed-population analysis of floods caused by monsoonal storms, frontal systems, and dissipating tropical cyclones. Assumptions: A, data are strictly stationary in time; B, discharge for 1983 flood is not considered as a historic peak; C, data are weakly stationary but are considered stationary for the indicated period, and future flood potential is similar with conditions in the period; D, floods caused by different storm types are assumed to be independent]

Years	Method	Assumptions	100-year discharge, in cubic meters per second	
			At Tucson	At Cortaro
All	MM	A,B	872	1,150
ENSO	MM	A,B	1,300	1,620
Non-ENSO	MM	A	628	746
All	ML,MP	A,B,D	1,050	1,610
1930–59	ML,MP	C,D	323	——
1960–86	ML,MP	B,C,D	1,660	2,030

tent storm types for the period of record on the Santa Cruz River, Hirschboeck's (1985) storm types were combined for this study into the three categories of monsoonal storms, synoptic-frontal systems, and dissipating tropical cyclones. Hirschboeck's (1985) monsoonal-local, monsoonal-widespread, and monsoonal-frontal types are classified simply as monsoonal storms. Widespread synoptic, fronts, and cutoff-low types are classified as synoptic-frontal systems. The tropical-storm type was redefined as a dissipating tropical cyclone using criteria of Smith (1986). Floods for 1915–86 were classified using these criteria independent of Hirschboeck's (1985) classification. Several discrepancies in the classification of floods caused by dissipating tropical cyclones occurred, mainly because the primary reference on tropical cyclones (Smith, 1986) was not available when Hirschboeck did her classification. The largest annual flood was then determined for each storm type.

A potential problem with dependence among storm types occurs because incursions of dissipating tropical cyclones are often associated with cutoff low-pressure systems. Cutoff low-pressure systems, which are lumped with synoptic-frontal systems, cannot be detected without 500-millibar height data. The chronology of tropical cyclones that is now available (Smith, 1986; Jose Arroyo Garcia and others, Circuito Exterior, Ciudad Universitaria, Mexico City, written commun., 1989), however, permits an unambiguous classification of floods caused by this storm type.

Patterns present in the time series of annual floods at Tucson caused by three storm types (fig. 19, table 8) indicate the cause for the shift in magnitude and seasonality of annual floods (fig. 2). The magnitude of floods caused by dissipating tropical cyclones and frontal systems increased after 1960 (fig. 19). The decadal frequency of floods above base discharge caused by dissipating tropical cyclones did not change after 1960 (2.9 per decade for 1960–84 compared with 3.0 per decade for 1930–59). Decadal frequency of floods above base caused by frontal systems, however, nearly doubled from 2.0 per decade in 1930–59, to 3.8 per decade in 1960–84. Although the magnitude of floods caused by monsoonal storms does not appear to change (fig. 19), the frequency decreases from 9.7 per decade in 1930–59 to 7.3 per decade after 1960. These results illustrate the inverse relation between the occurrence of floods caused by monsoonal storms and floods caused by dissipating tropical cyclones and frontal systems. Also, floods caused by different storm types in 1960–84 should be considered as populations distinct from those in 1930–59.

Methods of Flood-Frequency Analysis

Annual floods caused by different storm types can be analyzed as type I censored data. Censored data arise when a known number of observations are missing from a sample population (Cohn, 1986). Type I censoring occurs when all values larger than a fixed threshold, or censoring level, are observed and all values less than the censoring level are not (Cohn, 1986). The partial-duration series is determined by selecting a base discharge above which all discharges are determined. Therefore, a series that consists of the largest annual floods above base discharge and caused by a single storm type is, by definition, type I censored and independent data from a single population.

Plotting positions are assigned to the data using a generalized equation developed by Hirsch and Stedinger (1987) (Stedinger and others, 1988). Consider the case of one censoring level with record length (h) and number of floods (n) that exceed the censoring level (base discharge). Discharges that exceed the censoring level are ranked from largest to smallest by $i=1,2,3,\ldots,n$. The probabilities of discharges exceeding the censoring level are given by

$$p_i=(n/h)[(i-a)/(n+1-2a)],\ i=1,2,3,\ldots,n. \qquad (1)$$

In this report, we use a = 0.44 for Gringorten plotting positions (see Hirsch, 1987). The choice of plotting position is inconsequential because the differences among plotting position types are small compared with their sampling variability (Hirsch and Stedinger, 1987). The recurrence interval, T, for a flood is the inverse of p calculated with equation 1.

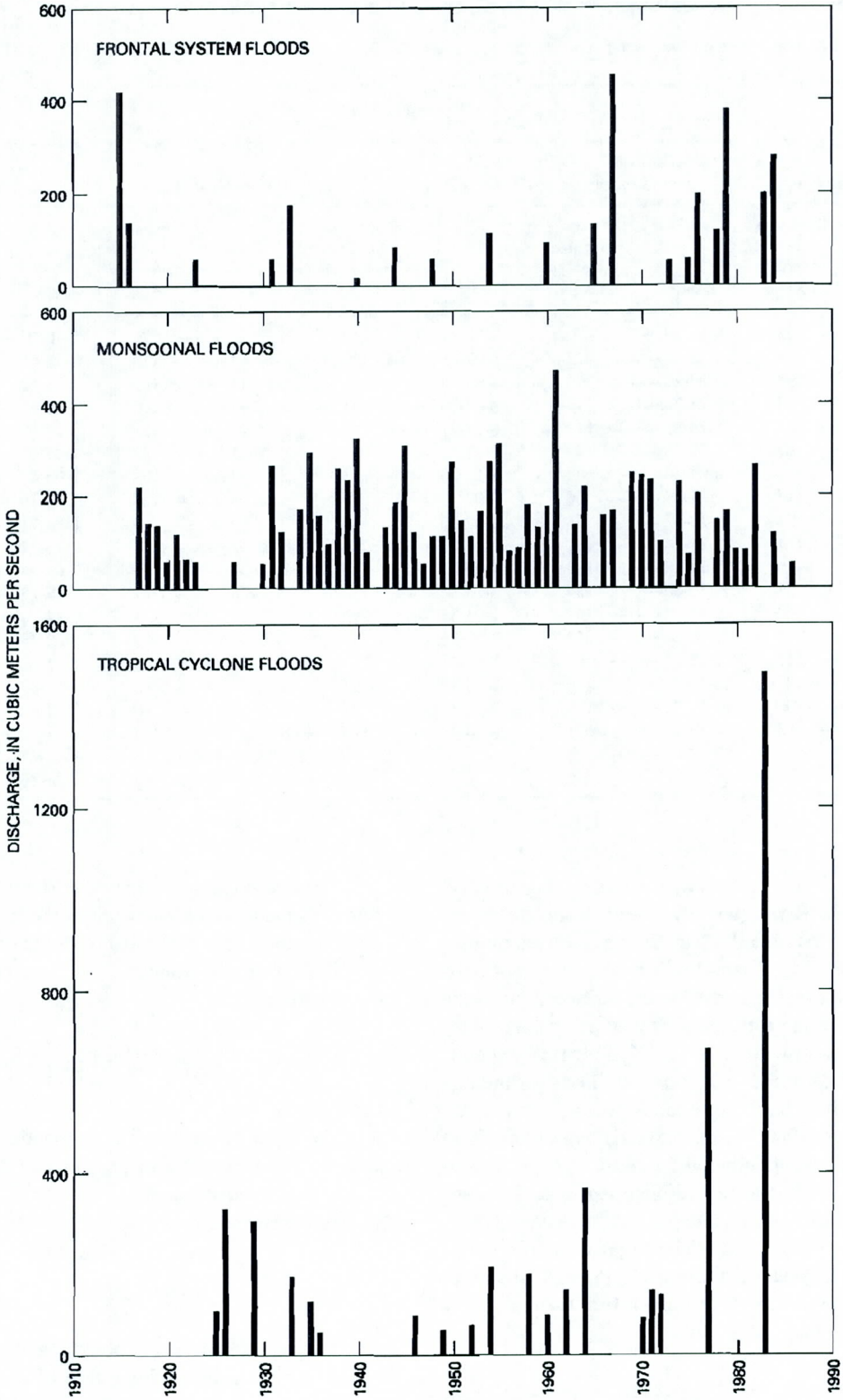

Figure 19. Largest annual floods at or above base discharge (48 m^3/s) on Santa Cruz River at Tucson caused by frontal systems, monsoonal storms, and dissipating tropical cyclones.

Table 8. Floods above base discharge, by storm type, Santa Cruz River at Tucson, Arizona

[Base discharge, 48 m^3/s. Hydroclimatic water year, November 1 to October 31]

Floods caused by									
Frontal storms		Dissipating tropical cyclones		Monsoonal storms					
Date	Discharge, in cubic meters per second	Date	Discharge, in cubic meters per second	Date	Discharge, in cubic meters per second	Date	Discharge, in cubic meters per second	Date	Discharge, in cubic meters per second
12-23-14	425	9-18-25	96	9-08-17	212	8-14-41	71	8-10-60	174
1-20-16	142	9-28-26	323	8-07-18	139	8-02-43	128	8-23-61	470
11-17-23	58	9-24-29	295	8-02-19	133	8-16-44	185	8-26-63	132
2-16-31	58	9-21-33	173	8-09-20	55	8-10-45	306	7-24-64	214
8-21-33	173	8-24-35	117	8-01-21	113	8-04-46	121	8-19-66	156
9-15-44	87	8-08-36	49	7-22-22	57	8-10-47	48	7-17-67	166
9-27-48	55	10-01-46	84	8-17-23	54	8-16-48	109	8-06-69	247
9-24-54	114	9-10-49	56	9-07-27	55	8-08-49	108	7-20-70	242
1-12-60	91	9-20-52	64	8-07-30	50	7-30-50	269	8-17-71	227
12-23-65	137	7-20-54	191	8-10-31	261	8-02-51	142	7-15-72	98
12-20-67	456	7-29-58	180	7-30-32	119	8-16-52	108	7-08-74	225
3-14-73	54	9-10-60	84	8-23-34	170	7-15-53	167	7-12-75	70
9-13-75	60	9-26-62	141	9-01-35	292	7-24-54	271	9-25-76	201
9-25-76	201	9-10-64	368	7-26-36	153	8-03-55	309	8-02-78	142
10-21-78	118	9-05-70	81	7-10-37	93	7-29-56	74	8-15-79	163
12-19-78	382	8-12-71	142	8-05-38	255	8-31-57	86	8-13-80	78
2-04-83	1200	10-19-72	133	8-03-39	227	7-29-58	180	7-27-81	76
12-28-84	283	10-10-77	671	8-14-40	320	8-20-59	125	8-23-82	[1]260
		10-02-83	1,493					8-14-84	113
								7-21-86	50

[1]Estimated.

The censored data for each hydroclimatic type of flood on the Santa Cruz River (table 9) were fit to the three-parameter log-Pearson type III distributions using maximum-likelihood analysis. The method of moments was not used because reliable estimates of the mean, variance, and skew of censored data are more efficiently made using maximum-likelihood analysis (Pollard, 1977, p. 245–246). Techniques used to fit type I censored data to probability distributions using maximum-likelihood techniques were presented by Stedinger and Cohn (1986, 1987). Stedinger and Cohn (1986) developed a maximum-likelihood function, L, for the combination of conventional gage and historical data. Because no historical data are used for the Santa Cruz River at Tucson, the likelihood function has to be slightly modified from those given in Stedinger and Cohn (1986) and Stedinger and others (1988). The likelihood function, L_N, for nonexceedances of base discharge is

$$L_N(\mu,\sigma,\gamma) = [F(X_b)]^{(h-n)}, \tag{2}$$

where

μ = population mean,
σ = population standard deviation,
γ = the population skew coefficient,
$F(X_b)$ = the cumulative-density function, and
X_b = logarithm (base 10) of the base discharge.

The likelihood function for discharges that exceed base discharge is

$$L_N(\mu,\sigma,\gamma) = \prod_{i=1}^{n}\left[f(x_i)\right], \tag{3}$$

where

$f(x_i)$ = the probability-density function, and
x_i = an array of the logarithms of floods that exceed base discharge.

The total likelihood function is

$$L(\mu,\sigma,\gamma)=L_N \bullet L_E. \tag{4}$$

Because equation 4 is maximized over μ, σ, and γ and the maximum of the logarithm of the likelihood function, ln L, occurs at the same place as the maximum for the likelihood function, L, equation (4) becomes

$$\ln L(\mu,\sigma,\gamma) = (h-n)\ln\left[F(X_b)\right] + \sum_{i=1}^{n}\ln\left[f(x_i)\right]. \tag{5}$$

Table 9. Floods above base discharge, by storm type, Santa Cruz River at Cortaro, Arizona

[Base discharge, 76 m³/s. Hydroclimatic water year, November 1 to October 31]

Floods caused by									
Frontal storms		Dissipating tropical cyclones		Monsoonal storms					
Date	Discharge, in cubic meters per second	Date	Discharge, in cubic meters per second	Date	Discharge, in cubic meters per second	Date	Discharge, in cubic meters per second	Date	Discharge, in cubic meters per second
12-31-40	482	7-16-54	173	8-14-40	482	8-12-58	224	7-12-75	147
9-16-44	122	7-29-58	206	8-08-41	170	8-20-59	227	9-25-76	300
9-10-46	79	9-26-62	317	9-24-43	156	8-11-60	182	9-10-77	133
3-23-54	143	9-10-64	450	8-16-44	160	8-16-84	146	8-02-78	79
1-09-57	78	9-06-70	136	8-10-45	397	8-23-61	416	7-25-81	118
10-28-59	79	10-19-72	255	8-04-46	126	8-26-63	205	8-23-82	377
1-12-60	176	10-10-77	651	8-15-47	213	9-06-64	203	8-07-83	176
12-22-65	476	10-02-83	1,841	7-30-50	365	7-16-65	77		
12-21-67	448	9-06-84	83	7-25-51	193	8-19-66	169		
2-22-73	104			8-14-52	173	7-17-67	163		
3-02-78	222			7-14-53	306	8-06-69	238		
12-18-78	533			7-24-54	259	7-20-70	317		
9-22-81	122			8-03-55	470	8-20-71	258		
9-11-82	190			7-29-56	89	8-12-72	200		
2-04-83	216			9-01-57	125	7-08-74	331		

Equation 5 is iteratively maximized by finding the point where $\partial(\ln L)/\mu$, $\partial(\ln L)/\partial\sigma$, and $\partial(\ln L)/\partial\gamma$ equal zero (Stedinger and others, 1988). Details of the numerical methods used to maximize equation 5 are given in Stedinger and Cohn (1986), Cohn (1986), and Stedinger and others (1988).

Mixed-population analysis is a method used to combine different populations of floods that may occur in a gaging record to estimate annual recurrence intervals for that river (Kite, 1988, p. 6–7). Distinct populations can be combined in several ways. One approach for estimating the cumulative density function, F_T, from m separate cumulative density functions, F_i, is given by Waylen and Woo (1982) as

$$F_T\left(X \le x\right) = \prod_{i=1}^{m} F_i\left(X \le x\right). \qquad (6)$$

This approach is difficult using maximum-likelihood analysis, because F would have to be differentiated and substituted into equations 2, 3, and 5 for solution. A similar method given by Kite (1988) and Crippen (1978) simply uses the assumption of independence of the populations to estimate the exceedance probability of occurrence. For two populations, the composite exceedance probability, P_T, is estimated using

$$P_T(X \ge x) = P_1(X \ge x) + P_2(X \ge x) - P_1 P_2, \qquad (7)$$

where $P_1(X \ge x)$ and $P_2(X \ge x)$ are the exceedance probabilities of the independent populations. Jarrett and Costa (1988) showed an example of two-population mixed-population analysis for Colorado. A third population can be introduced to produce

$$P_T(X \ge x) = P_1 + P_2 + P_3 - P_1P_2 - P_1P_3 - P_2P_3 + P_1P_2P_3 \qquad (8)$$

By substituting $1/T$ for P and rearranging, the annual recurrence interval for the mixed population, T_a, can be estimated as three populations described by T_1, T_2, and T_3 from

$$T_a = \frac{T_1T_2T_3}{(T_1T_2 + T_1T_3 + T_2T_3 - T_1 - T_2 - T_3 + 1)} \qquad (9)$$

Frequency of Floods Caused by Different Storm Types

Three scenarios of flood frequency were analyzed for the Santa Cruz River at Tucson. First, probability distributions were fit to all data for annual floods caused by each storm type (fig. 19). The moments of the fitted distribution are given in table 10. Flood-frequency relations (fig. 20) show the relative importance of each storm type to annual flood frequency. Floods caused by monsoonal storms dominate flood frequency for recurrence intervals of less than 10 years. Floods caused by tropical cyclones dominate flood frequency at recurrence intervals above 20 years. Although the frequency of floods caused by frontal systems never dominates (fig. 20), it parallels that for

tropical cyclones up to the 10-year recurrence interval, at which point the two relations diverge. The relation for the Santa Cruz River at Cortaro is similar.

The relations shown in figure 20 do not represent an accurate statistical analysis of flood frequency on the Santa Cruz River. As is apparent for floods caused by tropical cyclones and frontal systems, the frequency of floods caused by storm types is dependent on the period of record that is considered (fig. 19). Use of data from all periods for each storm type violates the assumption that a homogeneous population is being analyzed. The annual flood frequency for this scenario (fig. 20) is probably meaningless because flood frequency appears to exhibit weak stationarity of order 1. For comparative purposes, the 100-year flood estimated from a mixed-population analysis is 1,050 m^3/s at Tucson and 1,610 m^3/s at Cortaro.

To obtain stationary series for analysis, the assumption was made that populations of floods caused by frontal systems, dissipating tropical cyclones, and monsoonal storms are derived from different populations for 1930–59 and 1960–86. At Cortaro, only flows for 1960–84 were analyzed because only 18 years of data are available before 1960. The relations for floods at Tucson caused by different storm types that occurred after 1960 appear in figure 21. The same general relations occur as in figure 20, but discharges for given recurrence intervals are larger for the post-1960 relations (fig. 21). Comparison of the estimated mean, standard deviation, and skew coefficients

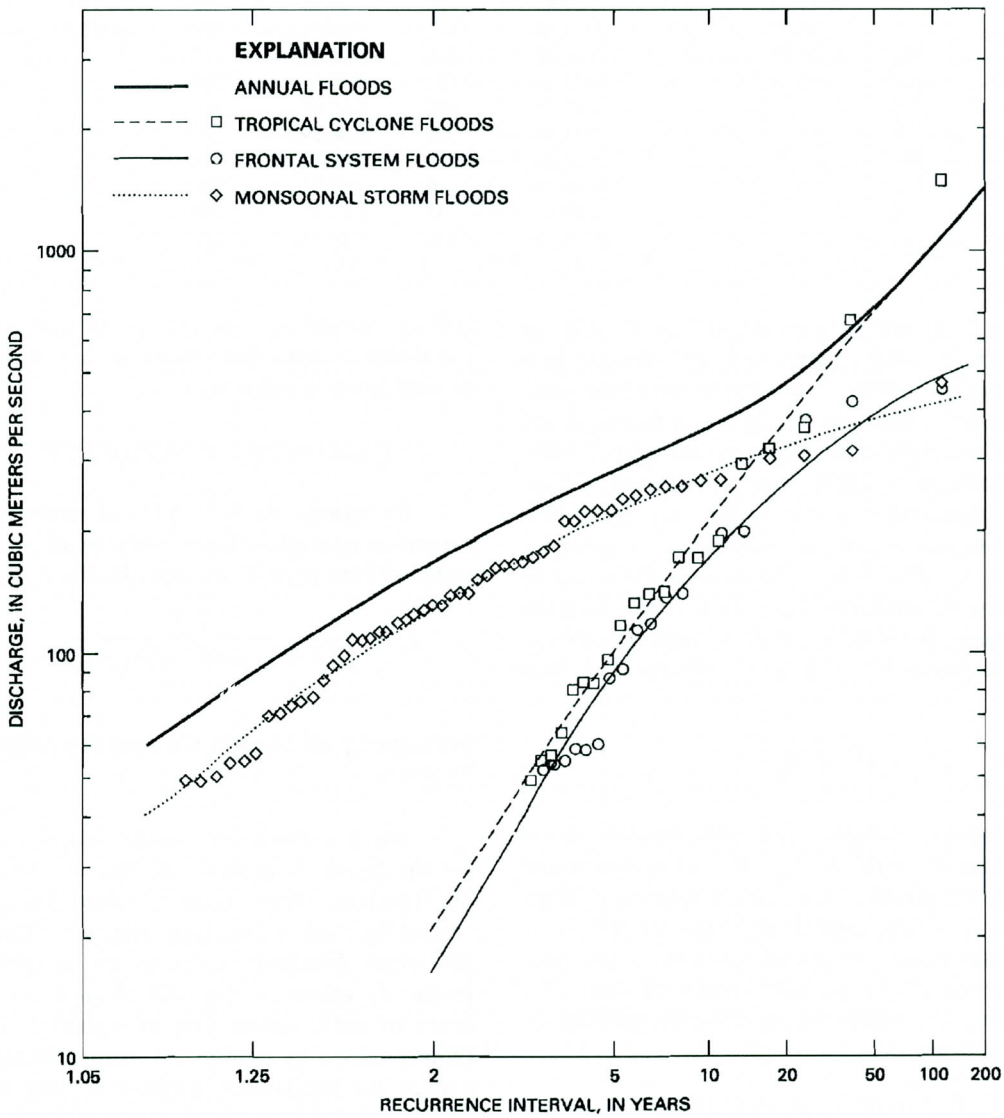

Figure 20. Mixed-population analysis of floods caused by different storm types between 1915 and 1986, Santa Cruz River at Tucson, Arizona. Probability distributions were fit using invalid assumptions; curves are presented for illustrative purposes only.

for post-1960 floods with those estimated for the entire record (table 10) suggests the reason for the increase. Although the mean discharge decreases for post-1960 floods at Tucson caused by tropical cyclones and monsoonal storms, the variances for all types increase. The skew coefficient becomes more negative (table 10), but because it is poorly estimated, changes in the skew coefficient are not considered significant. From mixed-population analysis, the annual 100-year flood for Santa Cruz River at Tucson is 1,660 m^3/s after 1960 (fig. 21). At Cortaro, the annual 100-year flood is 2,030 m^3/s after 1960. Both estimates are strongly affected by the large flood of October 1983.

Results for floods at Tucson for 1930–59 caused by tropical cyclones and frontal systems (fig. 22) contrast with the post-1960 results; floods caused by monsoonal storms dominate flood frequency. Although the means for floods caused by tropical cyclones and frontal systems are similar for 1930–59 and post-1960 (table 10), the standard deviations are much less for 1930–59 than post-1960. For 1930–59, the annual 100-year flood is 323 m^3/s and is essentially the frequency of floods caused by monsoonal storms (fig. 22).

The results of the hydroclimatic flood-frequency analysis underscore the cause for the increased flood frequency on the Santa Cruz River. The probability for floods caused by dissipating tropical cyclones, frontal systems, and, to a lesser extent, monsoonal storms changed in the 20th century. The greatest difference among the distributions estimated for 1930–59 and 1960–86 is the increased

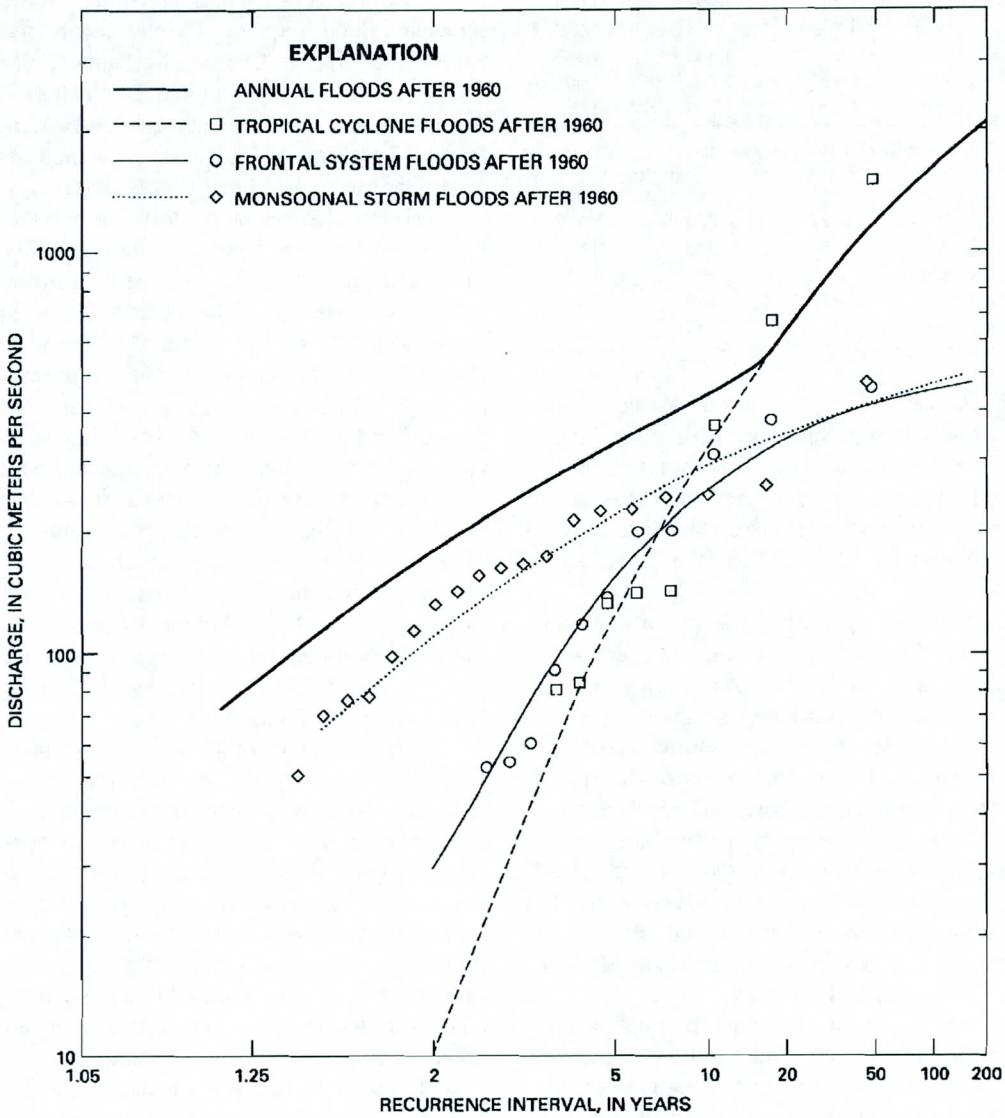

Figure 21. Mixed-population analysis of floods caused by different storm types between 1960 and 1986 for the Santa Cruz River at Tucson, Arizona.

Table 10. Statistics for annual series of floods caused by three storm types for the Santa Cruz River at Tucson and Cortaro, Arizona

[Statistics were generated by fitting floods above base discharges of 48 and 76 m^3/s for the Tucson and Cortaro stations, respectively, using maximum-likelihood analysis]

Floods caused by storm type	Mean logarithm of discharge	Standard deviation of log discharge	Coefficient of skew of log discharge
Santa Cruz River at Tucson, Arizona			
All tropical cyclones	1.264	0.865	–0.400
All frontal systems	1.007	1.118	–1.133
All monsoonal storms	2.068	.327	–.865
Tropical cyclones after 1960	.730	1.596	–1.040
Frontal systems after 1960	1.133	1.297	–1.639
Monsoonal storms after 1960	1.979	.423	–.948
Tropical cyclones, 1930–59	.586	1.442	–1.639
Frontal systems, 1930–59	.800	1.002	–1.501
Monsoonal storms, 1930–59	2.130	.298	–1.401
Santa Cruz River at Cortaro, Arizona			
All tropical cyclones	.523	1.651	–.948
All frontal systems	2.427	.884	–1.112
All monsoonal storms	2.214	.313	–1.080
Tropical cyclones after 1960	.778	1.675	–1.112
Frontal systems after 1960	1.218	1.296	–1.639
Monsoonal storms after 1960	2.147	.335	–1.174

variance and, in the case of floods caused by tropical cyclones and monsoonal storms, more negative skew coefficients. Because estimates of long-recurrence interval floods are heavily influenced by higher-order moments, the 100-year flood estimate for 1960–86 is more than four times larger than that for 1930–59 for the Santa Cruz River at Tucson.

The main problem with the hydroclimatic flood-frequency analysis is the inability to assign uncertainty estimates to discharges at given recurrence intervals. A method is not available for estimating standard errors or confidence limits for cumulative-distribution functions using mixed-population analysis. Variances for the floods caused by different storm types, however, are high, and the maximum length of a stationary period is only 30 years. For example, the uncertainty in the 100-year flood estimates from hydroclimatic-frequency analyses would be expected to be higher than for frequency analyses using a longer period of record, such as the 71-year annual flood series for Santa Cruz River at Tucson (fig. 2).

A second problem results from the assumption that floods during periods are derived from a stationary population. Climatic information suggests that transitions among periods may have been gradual instead of abrupt (fig. 10). The assumption of stationarity within periods is required to obtain estimates of population parameters, and no compelling evidence indicates problems with stationarity within the periods.

Finally, use of the hydroclimatic flood-frequency analyses requires an assessment of which period best represents future climatic conditions. Although no evidence was found to suggest that the conditions for 1960–86 have changed, the maximum length of periods examined in this study is only 30 years. The question of whether future conditions will be similar to 1930–59 or 1960–86 is impossible to answer at this time. It is also questionable that a meaningful 100-year discharge can be estimated from an annual flood series of only 30 years.

SUMMARY AND CONCLUSIONS

The effects of climatic variability on the annual flood series and flood-frequency estimates were evaluated for the Santa Cruz River at Tucson and Santa Cruz River at Cortaro. Previous estimates of the 100-year flood at Tucson, calculated using different techniques and assumptions, ranged from 572 to 2,780 m^3/s. This discrepancy has been attributed to increasing flood magnitudes caused by channelization and land-use changes in the last two decades. The magnitude of the 100-year flood for Santa Cruz River at Tucson, calculated from a log-Pearson type III distribution using the method of moments, increased from 577 to 872 m^3/s when annual peak discharges between 1970 and 1986 were included in the calculations. Flood-frequency estimates for the Santa Cruz River are strongly influenced by an extraordinary flood in October 1983, but it is also true that six of the seven largest floods at Tucson occurred after 1960. In addition, the seasonality of annual floods changed significantly after 1960; whereas floods in summer accounted for 97 percent of annual peaks between 1930 and 1959, floods in summer accounted for 61 percent of annual peaks between 1960 and 1986. Although changes in land use and channelization may have affected the magnitude of annual floods, climatic variability is identified as the main cause for the change in flood frequency.

The annual flood series at Tucson exhibits weak stationarity of order 1. Analyses for 1915–29, 1930–59, and 1960–86 showed that the mean does not change significantly; however, the variance and skew coefficient change significantly with time. Trend analyses revealed no trends in the annual flood series or among periods of the series. Trend analyses, however, are intended to detect changes in the mean instead of the variance. Changes in variance, which were detected in nonparametric tests, exert a heavy influence on estimates of long-recurrence interval floods such as the 100-year discharge.

In southern Arizona, fluctuations in large-scale oceanic and atmospheric processes are reflected in the seasonal distribution of precipitation and increased probability of large floods. Twentieth-century climatic variability

stems from decadal trends in atmospheric circulation over the Northern Hemisphere and in the frequency of El Niño-Southern Oscillation (ENSO) phenomena in the equatorial Pacific Ocean. Before 1930 and after 1960, westerly winds on average followed a more meridional path, and ENSO conditions occurred more frequently and with greater variability in the equatorial Pacific. By contrast, the westerlies followed a more zonal flow, and ENSO conditions occurred less frequently with less variability between 1930 and 1960. Meridional circulation and the climatology associated with ENSO conditions enhance Tucson precipitation in the winter, spring, and fall and possibly reduce summer rainfall.

Seasonal discharge on the Santa Cruz River is similarly related to climatic variability. Winter and fall floods account for 53 percent of annual peaks before 1930, only 3 percent from 1930 to 1959, and 39 percent after 1960. Changes in flood frequency on the Santa Cruz River are attributed to the changing probabilities of floods caused by certain storm types. In particular, the joint occurrence of cutoff low-pressure systems and tropical cyclones increases the probability for large floods along the Santa Cruz River. This joint occurrence tends to occur more frequently during ENSO years and during 1960–86.

Using procedures of the Interagency Advisory Committee on Water Data (1982), flood frequency at Tucson was estimated for the entire record using years with ENSO conditions and years with non-ENSO conditions. Climatic analyses suggest that the flood-producing mechanisms are not strictly stationary in the 20th century; therefore, analyses that require the assumption of stationarity may be invalid. Assuming stationarity for the entire record, the

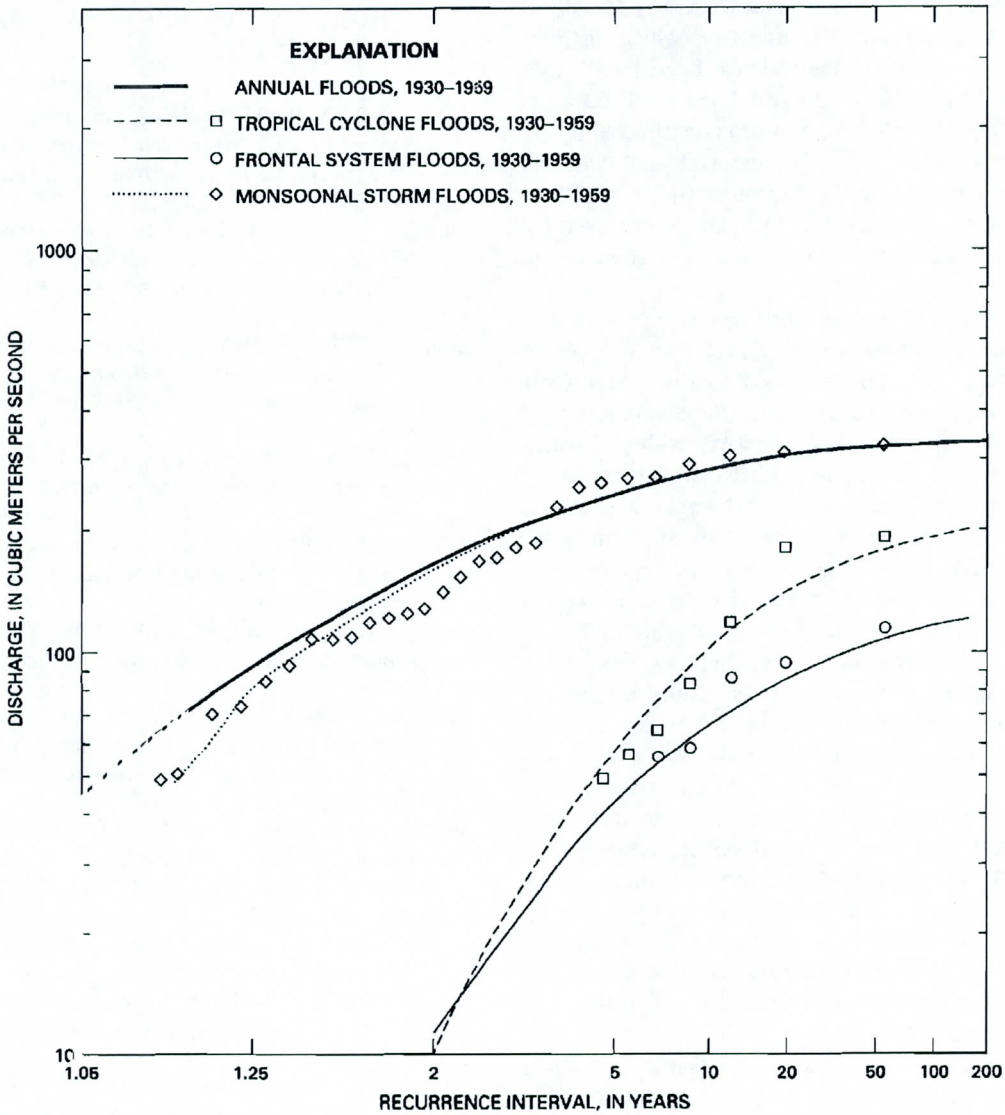

Figure 22. Mixed-population analysis of floods caused by different storm types between 1930 and 1959 for the Santa Cruz River at Tucson, Arizona

100-year flood is estimated to be 872 m^3/s. Assuming stationarity, the 100-year floods for years with ENSO and non-ENSO conditions are estimated to be 1,300 and 628 m^3/s, respectively. The frequency analysis for the entire record and for ENSO years is strongly affected by the unusually large flood of October 1983.

The frequency of floods caused by the three general storm types—summer monsoonal storms, frontal systems, and dissipating tropical cyclones—was estimated using maximum-likelihood analysis and the log-Pearson type III distribution. Annual flood frequency was estimated by assuming independence of the three types of floods and using a three-population mixed-population analysis. Floods caused by dissipating tropical cyclones determine the annual flood frequency at recurrence intervals greater than about 20 years for all years and for 1960–86. For 1930–59, floods caused by monsoonal storms dominate flood frequency for all recurrence intervals. Assuming stationarity, which analyses of climate suggest is invalid, the 100-year flood for all years is 1,050 m^3/s (table 7). The 100-year flood for 1960–86 is estimated to be 1,660 m^3/s and was strongly affected by the flood of October 1983. Likewise, the 100-year flood for 1930–59 was estimated to be 323 m^3/s (table 7). These analyses do not have an estimated uncertainty; however, the uncertainty is expected to be high because of short record length and high variance.

The results of flood-frequency analyses presented in this study raise questions about the validity of applying statistical flood-frequency analysis to the Santa Cruz River. Frequency analysis requires the assumptions of interannual independence and stationarity, neither of which are totally valid for the Santa Cruz River. Separation of the record into ENSO and non-ENSO conditions creates two independent populations but does not solve the problem of a variance that changes with time. Separation of floods by storm type assumes three independent, stationary populations, although long-recurrence-interval floods are estimated from stationary records of 30 years or less. Also, judicious use of the mixed-population results requires an assessment of future climatic conditions, which is questionable. Finally, separation of periods requires the assumption that climatic shifts are abrupt, whereas the climatic data presented in this report indicate that shifts may be gradual. Inclusion of the flood of October 1983 also adds to the complexity of the problem. Although this flood was the largest since at least 1891 and ordinarily would have been treated as a historic peak (Interagency Advisory Committee on Water Resources, 1982), considerations of stationarity prevented extension of a historical record length for this flood.

Flood-frequency estimates for the Santa Cruz River need to be used cautiously in design applications. Other methods, such as rainfall-runoff models (Ponce and others, 1985), may be appropriate alternatives to flood-frequency analysis. Frequency analysis, however, is appropriate in certain circumstances. For example, because ENSO conditions demonstrably affect flood frequency on the Santa Cruz River, flood plains could be managed for a specified recurrence interval of floods during ENSO conditions. Therefore, an appropriate estimate of the 100-year flood would be 1,300 m^3/s at Tucson. A similar scenario could be developed for floods caused by dissipating tropical cyclones. However, the period of record would have to be selected that best represents future or design conditions.

Perhaps the best estimate for the 100-year flood is obtained by assuming that future climate may be similar with that of 1960–86. This assumption may be valid for the immediate future but is tenuous when conditions for several decades into the future are considered. Given this assumption, an appropriate magnitude for the 100-year flood is 1,660 m^3/s at Tucson (table 7).

REFERENCES CITED

Aldridge, B.N., 1970, Floods of November 1965 to January 1966 in the Gila River basin, Arizona and New Mexico, and adjacent basins in Arizona: U.S. Geological Survey Water-Supply Paper 1850–C, 176 p.

Aldridge, B.N., and Eychaner, J.H., 1984, Floods of October 1977 in southern Arizona and March 1978 in central Arizona: U.S. Geological Survey Water-Supply Paper 2223, 143 p.

Aldridge, B.N., and Hales, T.A., 1984, Floods of November 1978 to March 1979 in Arizona and west-central New Mexico: U.S. Geological Survey Water-Supply Paper 2241, 149 p.

Andrade, E.R., and Sellers, W.D., 1988, El Niño and its effect on precipitation in Arizona: Journal of Climatology, v. 8, p. 403–410.

Baker, V.R., 1984, Questions raised by the Tucson flood of 1983: Journal of the Arizona-Nevada Academy of Sciences, v. 14, p. 211–219.

Balling, R.C., and Lawson, M.P., 1982, Twentieth century changes in winter climatic regions: Climatic Change, v. 4, p. 57–69.

Barry, R.G., Kiladis, G., and Bradley, R.S., 1981, Synoptic climatology of the western United States in relation to climatic fluctuations during the twentieth century: Journal of Climatology, v. 1, p. 97–113.

Betancourt, J.L., 1990, Tucson's Santa Cruz River and the arroyo legacy: Tucson, University of Arizona, doctoral dissertation, 239 p.

Betancourt, J.L., and Turner, R.M., 1988, Historic arroyo-cutting and subsequent channel changes at the Congress Street crossing, Santa Cruz River, *in* Whitehead, E.E., Hutchinson, C.F., Timmermann, B.N., and Varady, R.G., eds., Arid lands today and tomorrow: Boulder, Colorado, Westview Press, p. 1353–1371.

Boughton, W.C., and Renard, K.G., 1984, Flood frequency characteristics of some Arizona watersheds: Water Resources Bulletin, v. 20, p. 761–769.

Box, G.E.P., and Jenkins, G.M., 1971, Time series analysis: San Francisco, Holden-Day, 553 p.

Bradley, R.S., Diaz, H.F., Kiladis, G.N., and Eischeid, J.K., 1987, ENSO signal in continental temperature and precipitation records: Nature, v. 327, p. 497–501.

Burkham, D.E., 1981, Uncertainties resulting from changes in river form: American Society of Civil Engineers, Journal of the Hydraulics Division, v. 107, p. 593–610.

Carleton, A.M., 1986, Synoptic-dynamic character of "bursts" and "breaks" in the south-west U.S. summer precipitation singularity: Journal of Climatology, v. 6, p. 605–623.

———1987, Summer circulation climate of the American Southwest, 1945–1984: Annals of the Association of American Geographers, v. 77, p. 619–634.

Cayan, D.R., 1986, North Atlantic seasonal sea surface temperature anomalies and associated statistics: La Jolla, California, Scripps Institution of Oceanography, SIO Reference No. 85–19, 89 p.

Cohn, T.A., 1986, Flood frequency analysis with historical flood information: Ithaca, New York, Cornell University, doctoral dissertation, 144 p.

Conover, W.J., 1971, Practical nonparametric statistics: New York, John Wiley, 493 p.

Cooke, R.U., and Reeves, R.R., 1976, Arroyos and environmental change in the American Southwest: Oxford, England, Oxford University Press, 213 p.

Crippen, J.R., 1978, Composite log-type III frequency-magnitude curve of annual floods: U.S. Geological Survey Open-File Report 78–352, 5 p.

Cross, R.L., 1988, Eastern North Pacific hurricanes, 1987: Mariners Weather Log, v. 32, p. 12–16.

Diaz, H.F., and Quayle, R.G., 1980, The climate of the United States since 1895, Spatial and temporal changes: Monthly Weather Review, v. 108, p. 249–266.

Douglas, A.V., 1974, Cutoff lows in the southwestern United States and their effects on precipitation of this region: Tucson, Arizona, Laboratory of Tree Ring Research, Final Report on Department of Commerce Contract 1–35241 No. 3, 40 p.

Douglas, A.V., Cayan, D.R., and Namias, Jerome, 1982, Large-scale changes in North Pacific and North American weather patterns in recent decades: Monthly Weather Review, v. 110, p. 1851–1862.

Douglas, A.V., and Englehart, P.J., 1984, Factors leading to the heavy precipitation regimes of 1982–1983 in the United States, *in* Proceedings of the Eighth Annual Climate Diagnostics Workshop: Washington, D.C., National Oceanic and Atmospheric Administration, p. 42–54.

Dunne, Thomas, and Leopold, L.B., 1978, Water in environmental planning: San Francisco, W.H. Freeman, 818 p.

Durrenberger, R.W., and Wood, Richard, 1979, Climate and energy in the Tucson region: Tempe, Arizona State University, Laboratory of Climatology report, 90 p.

Dzerdzeevskii, B.L., 1969, Climatic epochs in the twentieth century and some comments on the analysis of past climates, *in* Wright, H.E., Jr., ed., Quaternary geology and climate, v. 16 of the Proceedings of the 7th Congress, International Quaternary Association: Washington, D.C., National Academy of Sciences Publication 1701, p. 49–60.

———1970, Circulation mechanisms in the atmosphere of the Northern Hemisphere in the 20th century: Moscow, Institute of Geography, Soviet Academy of Sciences, translated from the Russian by R. Goedecke, 361 p.

Eidemiller, D.I., 1978, The frequency of tropical cyclones in the southwestern United States and northwestern Mexico: Arizona State Climatologist, Climatological Publications, Scientific Papers 1, 41 p.

Elliott, W.P., and Angell, J.K., 1988, Evidence for changes in Southern Oscillation relationships during the last 100 years: Journal of Climate, v. 1, p. 729–737.

Enfield, D.B., 1989, El Niño, past and present: Reviews of Geophysics, v. 27, p. 159–187.

Eychaner, J.H., 1984, Estimation of magnitude and frequency of floods in Pima County, Arizona, with comparisons of alternative methods: U.S. Geological Survey Water-Resources Investigation 84–4142, 69 p.

Federal Emergency Management Agency, 1982, Flood insurance study, city of Tucson, Arizona, Pima County: Washington, D.C., Federal Emergency Management Agency, 45 p.

———1986, A unified national program for floodplain management: Washington, D.C., Federal Emergency Management Agency, Interagency Task Force on Floodplain Management, p. A-1 to D-12.

Folland, C.K., Palmer, T.N., and Parker, D.E., 1986, Sahel rainfall and worldwide sea temperatures, 1901–85: Nature, v. 320, p. 602–606.

Granger, O.E., 1984, Twentieth-century climate anomaly patterns over the southwestern United States: Physical Geography, v. 5, p. 164–185.

Hales, J.E., Jr., 1974, Southwestern United States summer monsoon source, Gulf of Mexico or Pacific Ocean?: Weatherwise, v. 24, p. 148–155.

Hansen, E.M., and Schwarz, F.K., 1981, Meteorology of important rainstorms in the Colorado River and Great Basin drainages: National Oceanic and Atmospheric Administration Hydrometeorological Report 50, 167 p.

Hansen, E.M., Schwarz, F.K., and Riedel, J.T., 1977, Probable maximum precipitation estimates, Colorado River and Great Basin drainages: National Oceanic and Atmospheric Administration Hydrometeorological Report 49, 161 p.

Hirsch, R.M., 1987, Probability plotting position formulas for flood records with historical information: Journal of Hydrology, v. 96, p. 185–199.

Hirsch, R.M., and Stedinger, J.R., 1987, Plotting positions for historical floods and their precision: Water Resources Research, v. 23, p. 715–727.

Hirschboeck, K.K., 1985, Hydroclimatology of flow events in the Gila River Basin, central and southern Arizona: Tucson, University of Arizona, doctoral dissertation, 335 p.

———1987, Catastrophic flooding and atmospheric circulation anomalies, *in* Mayer, Larry, and Nash, David, eds., Catastrophic flooding: Boston, Allen and Unwin, p. 23–56.

———1988, Flood hydroclimatology, *in* Baker, V.R., Kochel, R.C., and Patton, P.C., eds., Flood geomorphology: New York, John Wiley, p. 27–49.

Hjalmarson, H.W., 1987, Discussion—Large basin deterministic hydrology—A case study: American Society of Civil Engineers, Journal of the Hydraulics Division, v. 113, p. 1461–1463.

———1990, Flood of October 1983 and history of flooding along the San Francisco River, Clifton, Arizona: U.S. Geological Survey Water-Resources Investigations Report 85–4225–B, 42 p.

Horel, J.D., and Wallace, J.M., 1981, Planetary scale atmospheric phenomena associations with the Southern Oscillation: Monthly Weather Review, v. 109, p. 813–829.

Interagency Advisory Committee on Water Data, 1982, Guidelines for determining flood flow frequency: Washington, D.C., Interagency Advisory Committee on Water Data, Hydrology Subcommittee, Bulletin 17B, 28 p.

Jarrett, R.D., and Costa, J.E., 1988, Evaluation of the flood hydrology in the Colorado Front Range using precipitation, streamflow, and paleoflood data for the Big Thompson River basin: U.S. Geological Survey Water-Resources Investigations Report 87–4117, 37 p.

Kalnicky, R.A., 1974, Climatic change since 1950: Annals of the Association of American Geographers, v. 64, p. 100–112.

Keith, S.J.S., 1981, Stream channel recharge in the Tucson Basin and its implications for groundwater management: Tucson, University of Arizona, Master's thesis, 84 p.

Kiladis, G.N., and Diaz, H.F., 1989, Global climatic anomalies associated with extremes in the Southern Oscillation: Journal of Climate, v. 2, p. 1069–1090.

Kite, G.W., 1988, Frequency and risk analyses in hydrology, 4th edition: Littleton, Colorado, Water Resources Publications, 257 p.

Knapp, F.C., 1937, Report on Santa Cruz watershed: Tucson, Arizona, U.S. Department of Agriculture, Soil Conservation Service, unpublished report, 37 p.

Lewis, D.D., 1963, Desert floods—A report on southern Arizona floods of September 1962: Arizona State Land Department Water-Resources Report 13, 30 p.

Lins, H.F., 1985, Streamflow variability in the United States, 1931–78: Journal of Climate and Applied Meteorology, v. 24, p. 463–471.

Maddox, R.A., Canova, Faye, and Hoxit, L.R., 1980, Meteorological characteristics of flash flood events over the western United States: Monthly Weather Review, v. 108, p. 1866–1877.

Malvick, A.J., 1980, A magnitude-frequency-area relation for floods in Arizona: Tucson, University of Arizona, Engineering Experimental Station, Research Report 2, 25 p.

Mooley, D.A., and Parthasarathy, B., 1984, Fluctuations in all India summer monsoon rainfall during 1871–1978: Climatic Change, v. 6, p. 287–301.

Namias, Jerome, 1986, Persistence of flow patterns over North America and adjacent ocean sectors: Monthly Weather Review, v. 114, p. 1368–1383.

Namias, Jerome, Yuan, X., and Cayan, D.R., 1988, Persistence of North Pacific sea surface temperature and atmospheric flow patterns: Journal of Climate, v. 1, p. 682–703.

National Oceanic and Atmospheric Administration, 1988, Daily weather maps: National Oceanic and Atmospheric Administration, 8 p.

Nicholls, N., 1988, El Niño-Southern Oscillation and rainfall variability: Journal of Climate, v. 1, p. 418–421.

Ojo, Oyediran, 1987, Rainfall trends in West Africa, 1901–1985, *in* Solomon, S.I., Beran, M., and Hoff, W., eds., The influence of climate change and climatic variability on the hydrologic regime and water resources: International Association of Hydrological Sciences Publication No. 168, p. 37–43.

Pollard, J.H., 1977, A handbook of numerical and statistical techniques: Cambridge, England, Cambridge University Press, 349 p.

Ponce, V.M., Osmolski, Zbig, and Smutzer, David, 1985, Large basin deterministic hydrology, a case study: Journal of Hydraulic Engineering, American Society of Civil Engineers, v. 111, p. 1227–1245.

Pyke, C.B., 1972, Some meteorological aspects of the seasonal distribution of precipitation in the western United States and Baja California: Los Angeles, University of California, Water Resources Center Contribution No. 139, 205 p.

Quinn, W.H., Neal, V.T., Antunez de Mayolo, S.E., 1987, El Niño occurrences over the past four and a half centuries: Journal of Geophysical Research, v. 92, no. C13, p. 14449–14461.

Rasmusson, E.M., 1967, Atmospheric water vapor transport and the water balance of North America, part 1, Characteristics of the water vapor flux field: Monthly Weather Review, v. 95, p. 403–426.

———1984, El Niño, the ocean/atmosphere connection: Oceanus, v. 27, p. 5–12.

———1985, El Niño and variations in climate: American Scientist, v. 73, p. 168–177.

Reich, B.M., 1984, Recent changes in a flood series: Journal of the Arizona-Nevada Academy of Science, v. 14, p. 231–238.

Reich, B.F., and Davis, D.R., 1985, The 1983 Santa Cruz flood How should highway engineers respond?: Transportation Research Board Record, v. 1017, p. 1–7.

———1986, Reluctance to increase the regulatory flood on a degrading river: Phoenix, Arizona, Association of State Floodplain Managers, Inc., Proceedings of Seminar, "Improving the effectiveness of floodplain management in arid and semiarid regions", May 24–26, p. 99–102.

Reitan, C.H., 1960, Distribution of precipitable water vapor over the continental United States: Bulletin of the American Meteorological Society, v. 41, p. 79–87.

Reiter, E.R., 1983, Surges of tropical Pacific rainfall and teleconnections with extratropical circulation patterns, *in* Street-Perrott, F.A., Beran, M., and Ratcliff, R., eds., Variations in the global water budget: Dordrecht, Netherlands, D. Reidel, p. 285–299.

Reyes, Sergio, and Cadet, D.L., 1988, The southwest branch of the North American monsoon during 1979: Monthly Weather Review, v. 116, p. 1175–1187.

Roeske, R.H., 1978, Methods for estimating the magnitude and frequency of floods in Arizona: Arizona Department of Transportation ADOT–RS–15–121, 82 p. [Also available as NTIS report PB289 424].

Roeske, R.H., Garrett, J.M., and Eychaner, J.H., 1989, Floods of October 1983 in southeastern Arizona: U.S. Geological Survey Water-Resources Investigations Report 85–4225–C, 77 p.

Ropelewski, C.F., and Halpert, M.S., 1986, North American precipitation and temperature patterns associated with El Niño-Southern Oscillation (ENSO): Monthly Weather Re-

view, v. 114, p. 2352–2362.

Ropelewski, C.F., and Jones, P.D., 1987, An extension of the Tahiti-Darwin Southern Oscillation Index: Monthly Weather Review, v. 115, p. 2161–2165.

Rosendal, H.E., 1962, Eastern North Pacific tropical cyclones, 1947–1961: Mariners Weather Log, v. 6, p. 195–201.

Saarinen, T.F., Baker, V.R., Durrenberger, Robert, Maddock, Thomas, Jr., 1984, The Tucson, Arizona, flood of October 1983: Washington, D.C., National Academy Press, 112 p.

Schwalen, H.C.. 1942, Rainfall and runoff in the upper Santa Cruz River drainage basin: Tucson, University of Arizona, Agricultural Experiment Station Technical Bulletin No. 95, p. 421–472.

Sellers, W.D., 1960, Precipitation trends in Arizona and western New Mexico: Proceedings, 28th Annual Western Snow Conference, Santa Fe, New Mexico, p. 81–94.

Sellers, W.D., and Hill, R.H., eds., 1974, Arizona climate, 1931–1972: Tucson, University of Arizona Press, 616 p.

Slezak-Pearthree, M., and Baker, V.R., 1987, Channel change along the Rillito Creek system of southeastern Arizona, 1941 through 1983: Arizona Bureau of Geology and Mineral Technology Geological Survey Branch, Special Paper 6, 58 p.

Smith, Walter, 1986, The effects of eastern north Pacific tropical cyclones on the southwestern United States: National Oceanic and Atmospheric Administration Technical Memorandum NWS WS–197, 229 p.

Stedinger, J.R., and Cohn, T.A., 1986, Flood frequency analysis with historical and paleoflood information: Water Resources Research, v. 22, p. 785–793.

———1987, Historical flood frequency data: Its value and use, *in* Singh, Vijay, ed., Flood frequency and risk analysis: Boston, D. Reidel, p. 273–286.

Stedinger, J.R., Surani, Rafiq, and Therivel, Riki, 1988, Max users guide, A program for flood frequency analysis using systematic-record, historical, botanical, physical paleohydrologic and regional hydrologic information using maximum-likelihood techniques: Ithaca, New York, Cornell University Department of Environmental Engineering, 51 p.

Tang, M., and Reiter, E.R., 1984, Plateau monsoons of the northern hemisphere—A comparison between North America and Tibet: Monthly Weather Review, v. 112, p. 617–637.

Thomas, W.O., Jr., 1985, A uniform technique for flood-frequency analysis: Journal of Water Resources Planning and Management, v. 111, p. 321–337.

Troup, A.J., 1965, The Southern Oscillation: Quarterly Journal of the Royal Meteorological Society, v. 91, p. 490–506.

U.S. Army Corps of Engineers, 1972, Interim report on a survey for flood control, Santa Cruz River Basin: Los Angeles, U.S. Army Corps of Engineers Report, 43 p.

U.S. Water Resources Council, 1981, Guidelines for determining flood flow frequency: Hydrology Subcommittee Bulletin 17B, 183 p.

Waylen, Peter, and Woo, Ming-Ko, 1982, Prediction of annual floods generated by mixed processes: Water Resources Research, v. 18, p. 1283–1286.

White, N.D., and Garrett, W.B., 1987, Water resources data, Arizona, water year 1984: U.S. Geological Survey Water-Data Report AZ–84–1, 381 p.

Wilson, R.P., and Garrett, W.B., 1989, Water resources data, Arizona, water year 1987: U.S. Geological Survey Water-Data Report AZ–87–1, 385 p.

Wright, P.B., 1984, Relationships between indices of the Southern Oscillation: Monthly Weather Review, v. 112, p. 1913–1919.

Yarnal, B., and Diaz, H.F., 1986, Relationships between extremes of the Southern Oscillation and the winter climate of the Anglo-American Pacific Coast: Journal of Climatology, v. 6, p. 197–219.